

## Cosmic structure formation in hybrid inflation models

Richard A. Battye

*Department of Applied Mathematics and Theoretical Physics, University of Cambridge, Silver Street,  
Cambridge CB3 9EW, United Kingdom*

Jochen Weller

*Theoretical Physics Group, Blackett Laboratory, Imperial College, Prince Consort Road, London SW7 2BZ, United Kingdom*  
(Received 19 October 1998; published 24 January 2000)

A wide class of inflationary models, known as hybrid inflation models, may produce topological defects during a phase transition at the end of the inflationary epoch. We point out that, if the energy scale of these defects is close to that of grand unification, then their effect on cosmic structure formation and the generation of microwave background anisotropies cannot be ignored. Therefore, it is possible for structure to be seeded by a combination of the adiabatic perturbations produced during inflation and active isocurvature perturbations produced by defects. Since the two mechanisms are uncorrelated the power spectra can be computed by a weighted average of the individual contributions. We investigate the possible observational consequences of this with reference to general hybrid inflation models and also a specific model based on supergravity. These mixed perturbation scenarios have some novel observational consequences and these are discussed qualitatively.

PACS number(s): 98.80.Cq

### I. INTRODUCTION

The precise origin of cosmic structure is one of the most important questions facing cosmology today. Over the past 15 years there have been two competing paradigms: quantum fluctuations created during inflation [1]—a period of rapid expansion of the universe just after the Planck epoch which can solve the horizon and flatness problems of the standard hot big bang model—and perturbations generated by the gravitational effects of a network of topological defects [2–6], which may have formed during some cosmological phase transition close to the energy scale of a grand unification theory (GUT). In the case of inflation the fluctuations are generally adiabatic, Gaussian, and passive in the sense that once created they evolve in a deterministic way right up to the present day. These assumptions have simplified the process of making predictions in these models to the point where accurate ( $\sim 1\%$ ) calculations of the anisotropies in the cosmic microwave background (CMB) and the density fluctuations in cold dark matter (CDM) can be made for a given set of parameters in less than a minute on a modern workstation [7].

Making the predictions of the same level of accuracy for defect based models is much more difficult since the perturbations are isocurvature, non-Gaussian, and are created actively throughout the whole history of the universe, from the time of defect formation to the present day. However, recent work [8–12], has established a basis for future work on this subject defining what can be thought of as the standard model, although there still appears to be some room for understanding more subtle effects [12,13]. It was suggested in Refs. [9,10] that flat universe models with a critical matter density ( $\Omega_m=1$ ) normalized to the cosmic background explorer (COBE) would require unacceptably large biases ( $\approx 5$ ) between cold and baryonic matter on  $100h^{-1}$  Mpc scales to be consistent with the observed galaxy distribution,

but more acceptable models can be constructed in an open universe or one dominated by a cosmological constant [14–16], albeit with a bias of 2 relative to infrared astronomy satellite (IRAS) galaxies which are usually assumed to be good tracers of the underlying mass distribution. Since COBE normalized adiabatic models based on inflation have no problem producing the requisite amount of power on these scales, this suggests—if the data is shown to be accurate—that such models may at least be partially responsible for the formation of structure.

The idea of combining these two paradigms is a simple one since they are far from being mutually exclusive; very simply, if the inflationary reheat temperature is greater than the GUT scale then the post-inflationary universe will encounter phase transitions, which may form topological defects. More speculatively, one might form defects in a non-thermal phase transition induced by parametric resonance [17,18] during the reheating phase after inflation. But most cosmologists would prefer for there to be only a single source of fluctuations, based on some kind of “minimalist” principle, and would be skeptical of any theory which has both without further motivation. There are, however, a wide class of inflationary models, which may produce topological defects—usually assumed to be strings, although it is also possible to produce other kinds of defects—during a phase transition which marks the end of the inflationary epoch. These are known as hybrid inflation models [19]. Hence, there is sufficient motivation to consider mixed perturbation scenarios in which structure is formed by both adiabatic density fluctuations produced during inflation and active isocurvature perturbations created by defects [20], without breaking any principle of minimalism, and this is the subject of this paper.

In Sec. II we will discuss the individual components—the fluctuations generated by inflation and defects, in particular strings. The fact that there is no universal model of inflation

makes it difficult to make very specific predictions. Therefore, we will first treat hybrid inflation models in generality by reference to a simple model (see Ref. [21] for a compendium of inflationary models—both hybrid and otherwise), before discussing a specific model which was put forward recently to produce inflation in the context of supergravity [22]. We will concentrate specifically on mixing inflation with strings, since they are probably the most obvious candidate in these scenarios, but most of the general comments that we will make apply equally well to the case of other topological defects, for example, the global defect models considered in Ref. [8]. The models for strings that we will use are based on those already used in Refs. [9,10,13,15] and we will make two assumptions. First, we will make the simple assumption that the strings evolve in a perfect scaling regime, from their formation to the present day, and then we will attempt to incorporate the effects radiation-matter transition by use of the velocity dependent one scale model [23]. We should note that it is not our intention in choosing these particular models for inflation and strings to make any very specific predictions or claims as to their universal validity. Rather, we wish to discuss qualitatively the sort of phenomena one might possibly expect in the power spectra and their relation to the current and future observational data.

We will then discuss how the spectra can be combined in Sec. III. This is in fact trivial since the power spectra should be uncorrelated and hence the two can be combined by a weighted average. Clearly, the addition of this extra degree of freedom weakens any constraint that current observations place on each of the individual models and we will discuss this in four different contexts.

First, we consider general hybrid inflation models in which the relative amplitude of the adiabatic and string induced components is arbitrary, along with the spectral index (the initial density fluctuations created during inflation are normally assumed to have a simple power law form  $P(k) \propto k^n$ , where  $n$  is the spectral index). Specifically, we will comment on the constraints which come from analysis of the spectrum of CMB observations on large scales detected by COBE and also from their combination with measurements of the density fluctuations on small scales, which are normally quantified in terms of  $\sigma_8$ , the fractional over density in spheres with radius  $8h^{-1}$  Mpc. These are considered to be the most accurate and robust measurements in cosmology. Comparison to just the COBE data constrains the spectral index to be in the range  $|n-1| < 0.2$  [24], while a simple comparison of the amplitude of the CMB anisotropies with that of  $\sigma_8$  rules out the standard CDM scenario with  $n=1$  (see, for example, Ref. [25]), since the COBE normalized value of  $\sigma_8$  computed for this model is approximately twice that which is observed,  $\sigma_8^{\text{OBS}} \approx 0.6$  in a critical density universe whereas  $\sigma_8^{\text{CDM}} \approx 1.2$ , favoring a lower value of  $n \approx 0.8$ . But a more detailed joint analysis of all the available CMB data and measurements of  $\sigma_8$  [26,27] suggests that something close  $n=1$  gives a better fit to all the available data. Without performing a full likelihood analysis, we show qualitatively that these constraints can be relaxed since the large angle CMB can be induced by strings, allowing for higher spectral indices to fit the data usually at the expense

of the reducing the power on large scales. We will also consider models which use other cosmological parameters to fit the measurements of galaxy clustering on large scales ( $\approx 50-100h^{-1}$  Mpc). We should note that there still remains a strong upper limit on blue spectra since large spectral indices lead to the production of unacceptable numbers of primordial black holes [28].

We will then discuss the observational aspects of the specific model based on supergravity which is introduced in Sec. II B. In this case the relative normalization of the adiabatic and string induced components, and the spectral index, which in this case is also a function of scale, are fixed by a single parameter of the model. First, we show how the inclusion of the string component allows the more extreme values of this parameter, which give very blue spectra on large scales, to be more compatible with the relative amplitude of the COBE measurements and those of  $\sigma_8$ , than if it was absent. Then we show that simple modifications to the cosmological parameters can improve the fit to the shape of the observed matter power spectra on large scales.

Most speculatively, we examine the possibility that there may be interesting effects in the power spectrum on small scales. It has been suggested [29–31] that there is a feature in the power spectrum with wave number  $k \approx 0.1h \text{ Mpc}^{-1}$ , where the Hubble constant is given by  $H_0 = 100h \text{ km s}^{-1} \text{ Mpc}^{-1}$ , and such a feature in the power spectrum naturally occurs in these models, although not necessarily on these scales. We illustrate this possibility by reference to a number of simple examples, suggesting that the forthcoming redshift surveys [the Sloan digital sky survey (SDSS) and 2Df] should allow us to test this possibility more accurately. This feature in the matter power spectrum leads to more power on small scales than in pure adiabatic models and hence it might possible to effect the formation of damped Lyman- $\alpha$  systems and other early objects. We will discuss this in the context of the popular cold plus hot dark matter model which is thought to under produce such features.

The main focus of our discussion is to reconcile the amplitude of the COBE detection with the amplitude and shape of the observed galaxy distribution, a problem which both the standard CDM and defect models both suffer from. However, the near future will see an explosion in measurements of the CMB anisotropies over a wide range of scales, for example, from the microwave anisotropy probe (MAP) and Planck satellites. To this end, we finally discuss the implications for the CMB angular power spectra and the novel features which these models have, in particular the Doppler peak structure and non-Gaussianity. We will focus on the need to exclude or constrain these mixed perturbation scenarios.

## II. THE INDIVIDUAL FLUCTUATION SPECTRA

### A. General hybrid inflation models

The proto-typical model for hybrid inflation is one which includes two scalar fields  $\phi$ , a real scalar field known as the inflaton, and  $\psi$ , a complex scalar field which is coupled to the inflaton. The specific potential usually used is [19]

$$V(\phi, \psi) = \frac{1}{4\lambda}(M^2 - \lambda|\psi|^2)^2 + \frac{1}{2}m^2\phi^2 + \frac{1}{2}g^2|\psi|^2\phi^2, \quad (1)$$

where  $\lambda$  and  $g$  are dimensionless coupling constants, and  $M$  and  $m$  are the mass scales introduced; in particular  $M$  is that associated with spontaneous symmetry breaking, which in the case of  $\psi$  being a complex scalar field leads to the production of global strings at the end of inflation.

The massive part of the field  $\psi$  has an effective mass  $M(\psi)^2 = g^2\phi^2 - M^2$  and therefore for  $\phi > \phi_c = M/g$  there is a single minimum of the potential in the  $\psi$  direction at  $\psi = 0$ , whereas for  $\phi < \phi_c$  the potential develops minima with  $|\psi| = M/\sqrt{\lambda}$ . In the case where

$$M^2 \gg M_p m \sqrt{\lambda}, \quad M^2 \gg m^2/g^2 \quad (2)$$

and  $M_p$  is the Planck mass, inflation takes place for  $M_p > \phi > \phi_c$ , with the expansion being dominated by the vacuum energy  $V(0,0) = M^4/4\lambda$ , rather than the false vacuum. Hence, if the inflaton starts at around  $\phi \approx M_p$  as in the chaotic inflation scenario [32], then inflation takes place as it rolls down to  $\phi_c$ , at which point the field  $\psi$  falls down into the vacuum manifold creating strings. Of course the universe may continue to inflate after this point, at least partially diluting the defects, but if the phase transition takes place sufficiently late, which can always be arranged by an appropriate choice of the parameters, for example, by ensuring that  $M$  is greater than the Hubble parameter during inflation, then one will be left with a network of defects which will subsequently evolve toward a scaling regime.

The adiabatic density perturbations created in this model on a length scale  $l$  are given by [19]

$$\frac{\delta\rho}{\rho} = \frac{2\sqrt{6}\pi g M^5}{5\lambda\sqrt{\lambda}M_p^3 m^2} \left(\frac{l}{l_c}\right)^{-\beta^2}, \quad (3)$$

where  $l_c$  is the horizon size when the inflaton has value  $\phi_c$ ,  $\beta = m/\sqrt{3}H$  and

$$H^2 = \frac{2\pi M^4}{3\lambda M_p^2}, \quad (4)$$

is the Hubble parameter when  $\phi = \phi_c$ . This model has a spectral index  $n = 1 + 2\beta^2 > 1$ , and therefore if  $H \gg m$  then the spectrum is almost scale free, whereas if  $m \sim H$  then the spectral index can be much larger than one. In Ref. [19] two possible scenarios were considered. First, if  $g^2 \sim \lambda \sim 10^{-1}$  and  $m \sim 10^2$  GeV, then normalization to the observed fluctuations  $[(\delta\rho/\rho)_{\text{obs}} \sim 5 \times 10^{-5}$ , in these units] yields  $M \sim 10^{11}$  GeV, and hence the adiabatic density fluctuations will dominate over those produced by the strings  $[(\delta\rho/\rho)_{\text{str}} \sim GM^2 \sim 10^{-10}(\delta\rho/\rho)_{\text{obs}}]$ . In this case the creation of strings at this scale may have other interesting cosmological implications—the production of dark matter axions by the radiative decay of axions strings [33]—but they will not have a substantial effect on structure formation. However, if  $g \sim \lambda \sim 1$  and  $m \sim 5 \times 10^{10}$  GeV then normalization requires

that  $M \sim 10^{15}$  GeV—around the GUT scale—with a spectral index of  $n \approx 1.1$ . In this case the perturbations created by the strings must be taken into account since they are of comparable size to the adiabatic ones.

Since this simple model was first proposed, there have been many other hybrid inflation models discussed in the literature with a wide variety of predictions for the energy scale and spectral index, most of which adhere to the dogma that the natural scale for inflation is below the GUT scale and the perturbations are scale free (although, see Ref. [34]). However, this simple example stands as an illustration that simple models which create topological defects at the end of inflation exist and moreover the defects can be sufficiently massive to seed density perturbations which are of comparable size to the adiabatic perturbations created during inflation. In the next section we will discuss a particular model for hybrid inflation based on supersymmetry and supergravity which makes specific parameter based predictions for the energy scale and spectrum of initial fluctuations. These predictions will be used to illustrate the novel observational features of these mixed perturbation scenarios. We should, however, be mindful of the fact that no universally accepted model of inflation exists and many more models will be invented to try to reconcile the theoretical and observational prejudices of the day. Although many models will not have GUT scale defects as a generic consequence, it is a very natural scale for symmetry breaking transitions to occur and models which predict this are well worth investigating, even if their observational consequences appear, at first glance, to be at variance with the observations. In Sec. III B we will illustrate the effects of simple models with an arbitrary normalization, close to the GUT scale, and spectral indices which are not one, showing that, at least qualitatively, that they may be taken into account for some of the current observations.

### B. A specific inflation model based on supergravity

In the previous section we discussed the original hybrid inflation model, illustrating its salient features from the cosmological point of view. However, such a model does not have any particular motivation from the point of view of fundamental physics—the ultimate aim of these endeavors. Hence, for definiteness, we would like to have a specific model which has much stronger origins in the realm of high energy physics theories such as supergravity. There are a number of popular models which use the flat directions of superpotentials to allow slow-roll inflation, notably the F-term [36] and D-term [37] scenarios, some of which also produce topological defects during the phase transition at the end of inflation and could be candidates for the ideas that we are discussing here. However, we have chosen a model introduced by Linde and Riotto [22] to illustrate the qualitative nature of these scenarios. Although there are some subtle philosophical problems associated with this model [21], for a specific choice of the parameters it exhibits a number of the properties which we are interested in investigating. Here, we will derive the initial fluctuation spectrum for this model, following and extending the original work [22], and then we will incorporate the initial spectra into CMBFAST, the stan-

standard linear Einstein-Boltzmann solver, to compute the spectrum of CMB anisotropies and CDM. From now onwards we will work in units where the Planck mass appropriate for high energy physics applications, such as string theory, is given by  $(8\pi G)^{1/2} = 1$ .

The model is based on the simplest choice of the superpotential which takes the form [38]

$$W = S(\kappa\bar{\phi}\phi - \gamma^2), \quad (5)$$

where  $\phi$  and  $\bar{\phi}$  are conjugate pairs of chiral superfields,  $S$  is a neutral superfield and  $\kappa < 1$  is a parameter of the theory. If we canonically normalize the scalar field  $S = \sigma/\sqrt{2}$ , then the effective potential, excluding the D-term, is given by

$$V = \frac{\kappa^2|\sigma|^2}{2}(|\phi|^2 + |\bar{\phi}|^2) + |\kappa\bar{\phi}\phi - \gamma^2|^2. \quad (6)$$

For  $\sigma > \sigma_c = \gamma\sqrt{2/\kappa}$ , the mass of the chiral superfields is positive and the potential in their directions has a single minimum at  $\phi = \bar{\phi} = 0$ . Along this direction the potential is flat and so a viable inflationary model cannot be constructed. However, if one makes a slight modification to the potential it is possible, for example, by softly breaking supersymmetry (SUSY) [38]. The novel aspect of the Linde-Riotto model is that they suggested this may be done by the inclusion of radiative and supergravity corrections. In this case, if the field  $\sigma$  starts at some large value as in the chaotic inflation scenario and the original hybrid inflation model, then inflation takes place until the field rolls down to  $\sigma = \sigma_c$ , at which point the field will quickly roll down to the absolute minimum of the potential where  $\sigma = 0$  and  $\phi = \bar{\phi} = \gamma/\sqrt{\kappa}$ , producing topological defects if the vacuum manifold has non-trivial homotopy. It was suggested in Ref. [22] that such models can naturally have the correct symmetry breaking schemes to form cosmic strings and that the energy scale of these strings is given by  $\gamma/\sqrt{\kappa}$  which for an appropriate choice of parameters could be the GUT scale.

In order to compute the potential, therefore, we must include radiative effects and supergravity corrections. The one loop SUSY potential for this model is given by [39,40]

$$V_1 = \frac{\kappa^2}{128\pi^2} \left[ (\kappa\sigma^2 - 2\gamma^2)^2 \ln \frac{\kappa\sigma^2 - 2\gamma^2}{\Lambda^2} + (\kappa\sigma^2 + 2\gamma^2)^2 \ln \frac{\kappa\sigma^2 + 2\gamma^2}{\Lambda^2} - 2\kappa^2\sigma^4 \ln \frac{\kappa\sigma^2}{\Lambda^2} \right], \quad (7)$$

where  $\Lambda$  is the renormalization scale which is introduced in the usual way. Since the period of inflation that we are interested in takes place for  $\sigma \gg \sigma_c$ , one can expand this correction to the potential as

$$V_1 = \gamma^4 \frac{\kappa^2}{8\pi^2} \ln \frac{\sigma}{\sigma_c} + \dots \quad (8)$$

If the field is very large at the beginning of inflation then supergravity corrections will also be important. The supergravity (SUGRA) correction to the potential is given by

$$V_{\text{SUGRA}} = \gamma^4 \exp\left(\frac{\sigma^2}{2}\right) \left[ 1 - \frac{\sigma^2}{2} + \frac{\sigma^4}{4} \right] - \gamma^4 = \gamma^4 \frac{\sigma^4}{8} + \dots, \quad (9)$$

and hence by combining the two one gets the fully corrected approximate potential

$$V = \gamma^4 \left( 1 + \frac{\kappa^2}{8\pi^2} \ln \frac{\sigma}{\sigma_c} + \frac{\sigma^4}{8} \right), \quad (10)$$

which is strictly valid for  $\sigma \gg \sigma_c$ , but should also be useful for smaller values of  $\sigma$  close to  $\sigma_c$ .

Using this potential one can compute the evolution of the scalar field, which we have done in terms of  $N$  the number of  $e$ -foldings until the end of inflation. During the inflationary epoch  $3H^2 = V$  and  $3H\dot{\sigma} = -V'$ , from which we can deduce that  $\dot{\sigma}/H = -V'/V$  and hence

$$\frac{d\sigma}{dN} = \frac{V'}{V}, \quad (11)$$

since the scale factor  $a \propto e^{-N}$ . If we assume that the potential does not change appreciably during the early stages of inflation when the cosmologically interesting perturbations are being created, then one can solve the equation for the field  $\sigma$  in terms of  $N$ ,

$$\sigma^2 = \frac{\kappa}{2\pi} \frac{\frac{2\pi}{\kappa} \sigma_{\text{end}}^2 + \tan\left(\frac{\kappa}{2\pi} N\right)}{1 - \frac{2\pi}{\kappa} \sigma_{\text{end}}^2 \tan\left(\frac{\kappa}{2\pi} N\right)}, \quad (12)$$

where  $\sigma_{\text{end}}$  is the value of the field when inflation ends, that is, when  $N=0$ . Assuming this value of the field to be relatively small, which may not always be the case, one can further approximate (12) to give

$$\sigma \approx \sqrt{\frac{\kappa}{2\pi} \tan\left(\frac{\kappa}{2\pi} N\right)}. \quad (13)$$

From this we can see that there is a constraint on the value of the parameter  $\kappa$  from the requirement that there have been at least 60  $e$ -foldings, so as to make the universe almost flat by the present day. The argument of the tangent function should never be allowed to be greater than  $\pi/2$ , and hence one can deduce that  $\kappa < \kappa_c = \pi^2/60 \approx 0.16$ . The number of  $e$ -foldings  $N$  can then be related to the wavelength or wave number of the perturbations ( $l = 2\pi/k$ ) by

$$N \approx 54 - \ln\left(\frac{k}{1 h \text{ Mpc}^{-1}}\right) \approx 52 + \ln\left(\frac{l}{1 h^{-1} \text{ Mpc}}\right), \quad (14)$$

where we have assumed that the size of the universe is  $3000h^{-1} \text{ Mpc}$  at the present day and hence we can compute parametrically the field  $\sigma$  as a function of the comoving scale during inflation.

The spectrum of primordial density fluctuations generated by the evolution of this field during inflation can be approximated by

$$\frac{\delta\rho}{\rho} \approx \frac{\sqrt{3}}{5\pi} \frac{V^{3/2}}{V'} \approx \frac{\sqrt{3}}{5\pi} \gamma^2 \left( \frac{\kappa^2}{8\pi^2} \frac{1}{\sigma} + \frac{1}{2} \sigma^3 \right)^{-1}, \quad (15)$$

and spectral index, which is now scale dependent, is given by

$$n-1 \approx 2 \frac{V''}{V} = \left( 3\sigma^2 - \frac{\kappa^2}{4\pi^2} \frac{1}{\sigma^2} \right). \quad (16)$$

Clearly, the spectrum is not totally scale invariant since the field evolves according to Eq. (12) during inflation and in general the effective spectral index increases as one approaches the largest scales, but we now have a simple parametric formula which allows us to compute the initial spectrum of density fluctuations  $P_i(k)$ . One might also expect such models to create a tensor contribution to the CMB fluctuations on large scales, but this would be proportional to  $V^{1/2}$  and hence  $(\delta T/T)_T = \mathcal{O}(1) \gamma^2$ , which in the regime under consideration here is much smaller than that due to scalars [41].

Assuming that these adiabatic perturbations are the only contribution to the scales probed by COBE, one can use the normalization [42]

$$5.3 \times 10^{-4} \approx \frac{V^{3/2}}{V} \Big|_{\sigma=\sigma_{60}} \approx \gamma^2 \sigma_{60} \left( \frac{\kappa^2}{8\pi^2} + \frac{1}{2} \sigma_{60}^4 \right)^{-1}, \quad (17)$$

where  $\sigma_{60}$  is the value of the inflaton field when the current observable universe leaves the horizon during inflation. Therefore, using Eq. (13) one can deduce that

$$1.7 \times 10^{-5} \approx \frac{\gamma^2}{\kappa^{3/2}} \left[ \sin\left(\frac{30\kappa}{\pi}\right) \right]^{1/2} \left[ \cos\left(\frac{30\kappa}{\pi}\right) \right]^{3/2}, \quad (18)$$

and hence if  $\kappa$  is small, for example  $\kappa=0.08$ , then the symmetry breaking scale for the strings is given by  $\gamma/\sqrt{\kappa} \approx 2.3 \times 10^{-3}$ . If the phase transition which takes place at the end of inflation leads to the formation of strings, then their mass per unit length will be

$$G\mu \approx \frac{\gamma^2}{8\pi\kappa} \approx 2.1 \times 10^{-7}. \quad (19)$$

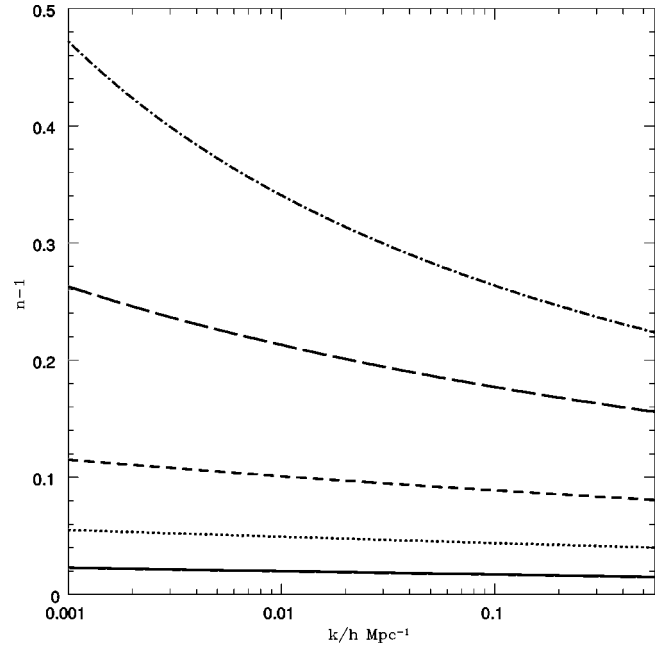


FIG. 1. The effective spectral index as function of the comoving scale during inflation for  $\kappa=0.08$  (solid line),  $\kappa=0.1$  (dotted line),  $\kappa=0.12$  (short dashed line),  $\kappa=0.13$  (long dashed line),  $\kappa=0.14$  (dot-short dashed line), and  $\kappa=0.15$  (dot-long dashed line).

Whereas, if  $\kappa$  is close to  $\kappa_c$ , for example  $\kappa=0.15$ , then one can deduce that  $G\mu \sim 5 \times 10^{-6}$ . In both cases the strings are around the scale at which they will also contribute substantially to the the COBE normalization and clearly they must be taken into account. In Sec. III C, we will discuss the implications of this for the relative contribution of adiabatic and string induced perturbations, and hence the computed spectra. For the moment we will ignore the strings and compute the spectrum of CMB anisotropies and fluctuations in the CDM, assuming that the adiabatic fluctuations are the only contribution.

The spectrum of initial fluctuations in this model is not a simple power law, and hence the spectral index is now a function of  $k$ , that is,  $P_i(k) \propto k^{n(k)}$ . The effective spectral index is plotted in the cosmologically interesting range of  $k$  for various values of  $\kappa$  in Fig. 1. For  $\kappa \leq 0.13$ , the spectral index is approximately constant, but for larger values of  $\kappa$  the spectrum rises sharply on large scales (small  $k$ ). This novel feature of the spectrum makes this model particularly interesting from the point of view of this paper since it will lead to a heavily blue shifted spectrum on very large scales and such a spectrum is tightly constrained by the observations. However, if the large angle part of the CMB spectrum is created by the strings then it may yet be possible for this model to be viable.

Now that we have derived the power spectrum of initial density fluctuations, it can be incorporated into CMBFAST in order to compute the power spectra of CMB anisotropies and matter fluctuations in the CDM which we would observe today for a given value of  $\kappa$ . The spectra are presented in Fig. 2 for various values of  $\kappa$  and the standard cosmological

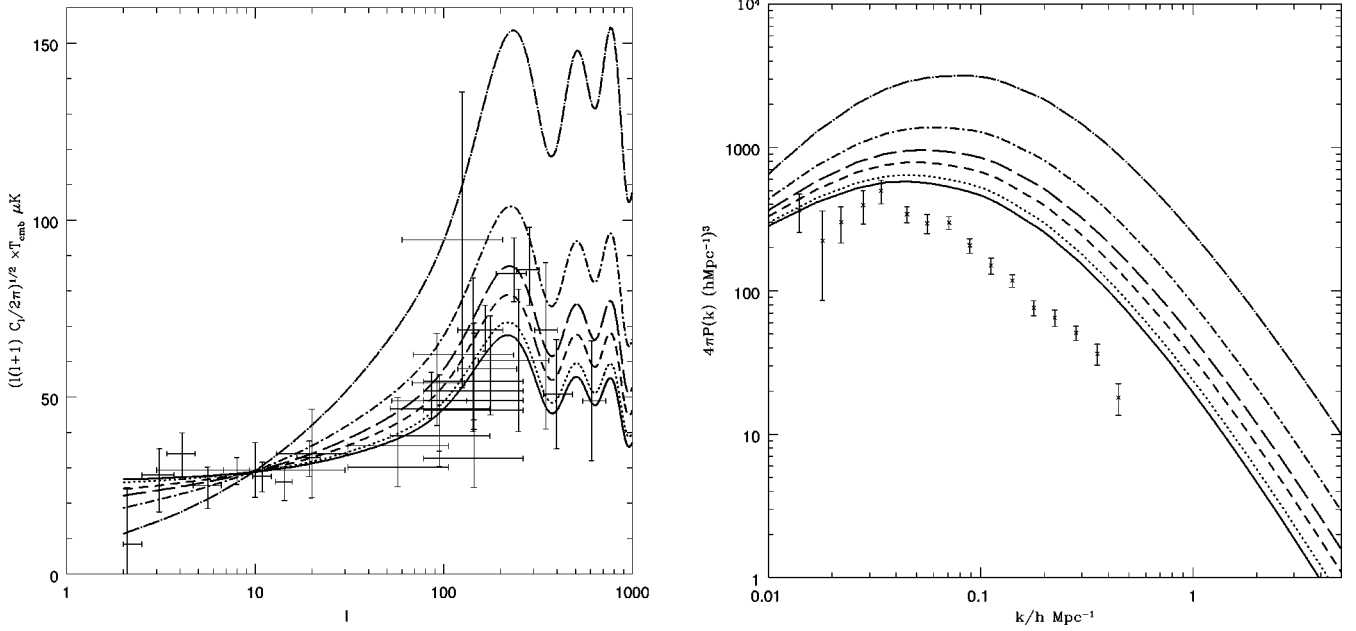


FIG. 2. On the left the angular power spectrum of CMB anisotropies and on the right the power spectrum of fluctuations in the CDM for the Linde-Riotto model without a string induced component, using the standard cosmological parameters and  $\kappa=0.08$  (solid line),  $\kappa=0.1$  (dotted line),  $\kappa=0.12$  (short dashed line),  $\kappa=0.13$  (long dashed line),  $\kappa=0.14$  (dot-short dashed line), and  $\kappa=0.15$  (dot-long dashed line). In both cases the current observational data points are also included to guide the eye. Notice that the CMB anisotropies for  $\kappa=0.15$  are wildly at odds with the observations at all scales and that even the models with smaller values of  $\kappa$  are clearly at odds with the amplitude and shape of the observed matter power spectrum.

parameters,<sup>1</sup> and the corresponding values of  $\sigma_8$  are tabulated in Table I. If  $\kappa$  is small (for example,  $\kappa \approx 0.08$ ) then the initial fluctuations are almost scale invariant and the results are essentially just those for standard CDM, but as  $\kappa$  increases the spectrum develops a tilt toward smaller scales, this being most graphically illustrated by the extreme case of  $\kappa=0.15$  where there are almost exactly 60  $e$ -foldings of inflation. When compared to the current observations [43–45], it is clear, just by inspection, that as they stand the models with larger values of  $\kappa$  would be ruled out by the observations of the CMB and galaxy correlations on small scales.

### C. String models

We have chosen strings as an example of topological defects produced at the end of inflation due to the well established property [46–49] that they evolve toward a self-similar scaling regime, in which the large scale properties of the network are described by a single scale and the density remains constant relative to the horizon. It is this property which makes them a possible source of an almost scale invariant spectrum of density perturbations across a wide range of scales, and hence a realistic model for structure formation. We could, of course, have used other topological defect

models, for example, the global defect models used in Ref. [8] and the qualitative predictions would be very similar. We should note that in doing this we have made the assumption that the initial distribution of strings is such that the network can achieve a scaling regime before the cosmologically interesting scales come inside the horizon. We have already pointed out that if a substantial period of inflation were to take place after the phase transition, then the strings would become diluted possibly radically altering the standard picture of string evolution. But, so long as inflation ends quickly enough, which is usually possible by tuning parameters, this dilution can be reversed before the cosmologically interesting epoch, just before the time of radiation-matter equality.

The particular model we will use to describe the two-point correlation functions of the strings is that which was developed in Refs. [50,9,10], where the string network is modeled as an ensemble of straight segments each with size  $\xi\eta$ , where  $\eta$  is the conformal time, and a random velocity chosen from a Gaussian distribution which has zero mean and variance  $v$ . The scaling regime is usually achieved by the production of loops and subsequent emission of radiation into the preferred channel, usually assumed to be gravita-

TABLE I. The computed values of  $\sigma_8$  for the Linde-Riotto model of inflation using the standard cosmological parameters, and a varying the parameter  $\kappa$ . Note that we have not included the possible effect of strings at this stage.

$\kappa$	0.08	0.10	0.12	0.13	0.14	0.15
$\sigma_8$	1.26	1.37	1.61	1.85	2.39	4.04

<sup>1</sup>The standard cosmological parameters used here and throughout this paper, unless stated otherwise, are a universe comprising of 95% CDM and 5% baryons, with three massless neutrinos, a Hubble constant  $H_0=50 \text{ km s}^{-1} \text{ Mpc}^{-1}$  and the standard recombination history.

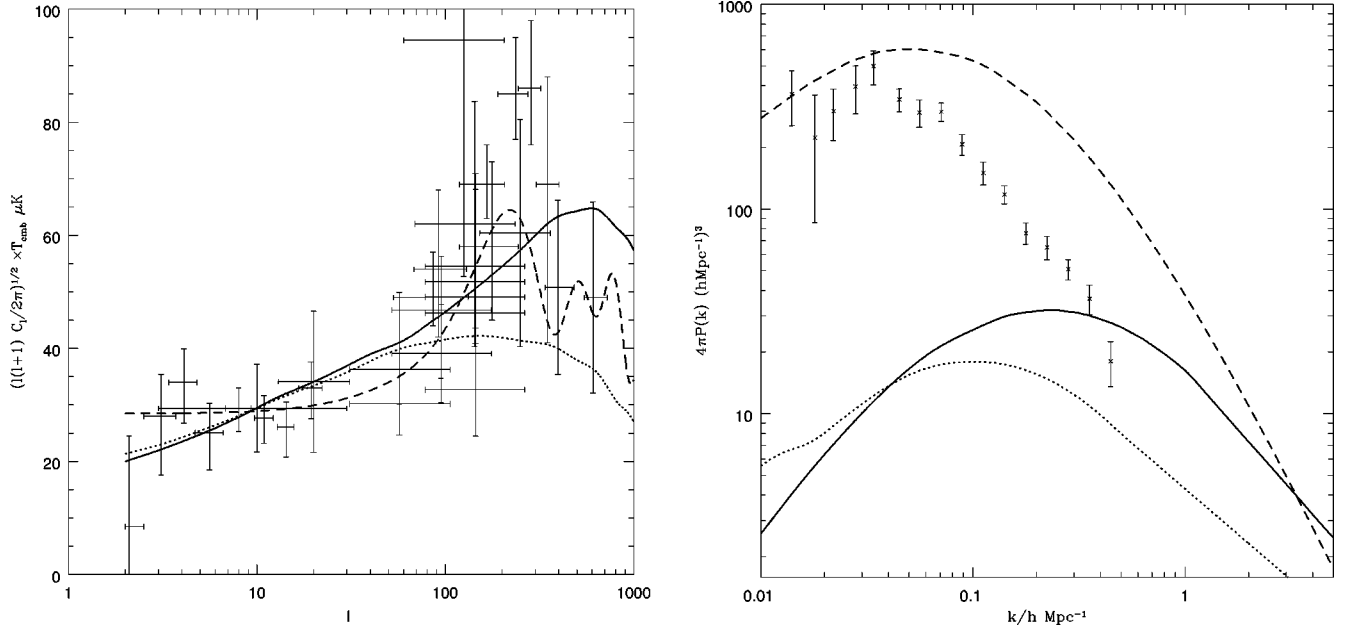


FIG. 3. On the left the angular power spectrum of CMB anisotropies and on the right the power spectrum of fluctuations in the CDM for the standard scaling source (dotted line) and the standard string model (solid line). In both cases the standard cosmological parameters have been used. The current observational data points and the equivalent spectra for the standard CDM scenario (short dashed line) are also included as a guide to the eye.

tional radiation. As a first approximation this can be accounted for by removing string segments at a rate which exactly maintains scaling. The results of using this approximation, which we shall call the standard scaling source, are presented in Fig. 3 along with some data points which represent the observations. The main qualitative features of this model are the apparent absence of any kind of Doppler peak in the CMB anisotropies and a matter power spectrum which on large scales ( $\approx 100h^{-1}$  Mpc) appears to require a bias of around 5 and the computed value of  $\sigma_8 \approx 0.31$ .

In order to model a network of strings more realistically one can do two things. First, one must attempt to take into account the effects of the matter radiation transition; scaling is a balance between the rate of expansion of the universe and the efficiency by which the network can lose energy into loops. During the transition era, that is,  $0.1\eta_{\text{eq}} < \eta < 100\eta_{\text{eq}}$ , where  $\eta_{\text{eq}}$  is the conformal time of equal matter radiation, the expansion rate is relaxing from the radiation era, where the scale factor is proportional to  $\eta$ , to the matter era, where it is proportional to  $\eta^2$ . Clearly, the nature of the scaling changes during this time and it has been suggested [23] that the change in the density of strings observed in the two different eras can be modeled using the velocity dependent one-scale model. This model treats the two parameters,  $\xi$  and  $\nu$ , used in construction of the two point functions as being dependent on the conformal time, allowing one to compute the rate at which the density changes.

Another aspect of string evolution which is not described by this simple model is the effect of small-scale structure. In high resolution simulations [47–49], it was found that small-scale structure built up close to the resolution of the simulation due to the copious production of loops on these scales. Although in reality this will be stabilized by radiation back-

reaction, some structure will remain effectively renormalizing the mass per unit length of these string segments to be  $\tilde{\mu} \approx 2\mu$ , where  $\mu$  is the ‘bare’ mass per unit length. Formally, this can be done by using a transonic equation of state for the string [52], that is, treating the strings as having a more complicated equation of state, rather than the usual Nambu-Goto one, where the energy per unit length and the tension are equal. In Minkowski space, the energy momentum tensor for a general string is

$$T_{\mu\nu}(x) = \int d\sigma \delta^4(x - X(\sigma, t)) [U \dot{X}_\mu \dot{X}_\nu - T X'_\mu X'_\nu], \quad (20)$$

where  $X^\mu(\sigma, t)$  are the spacetime coordinates of the string at time  $t$  parametrized by  $\sigma$ , some arbitrary coordinate along the string,  $U$  is the energy density of the string, and  $T$  is its tension. For the special case of a Nambu-Goto string the equation of state is  $T=U=\mu$ , but for the transonic case under discussion here  $TU=\mu^2$  and, therefore, if  $U=\tilde{\mu} \approx 2\mu$  then  $T/U \approx 1/4$ . By making this simple modification to the original model, one can incorporate some of the effects of small-scale structure. In particular, these modifications can lead to an enhanced peak structure due to the effects of an enhanced Newtonian potential [51]. A detailed investigation of these effects is the subject of work in progress.

Using the modifications described above, we have computed the spectra of CMB anisotropies and fluctuations in the CDM for the standard set of cosmological parameters and the results are also presented in Fig. 3. The main qualitative features of this model, which we will call the standard string model, are a slightly tilted spectrum of CMB anisotropies which rises to a single broad peak around  $l=400-600$  with

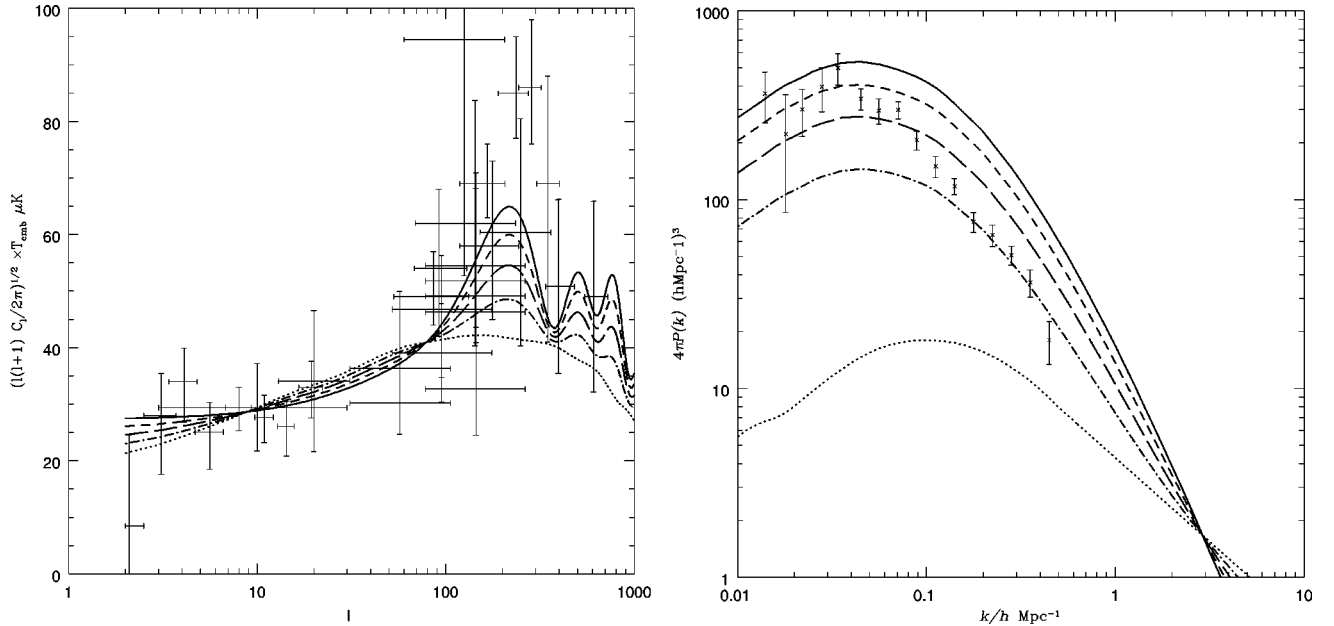


FIG. 4. On the left the angular power spectrum of CMB anisotropies and on the right the power spectrum of fluctuations in the CDM for the standard CDM scenario mixed with standard scaling source using a ratio of  $\alpha = 1.0$  (solid line),  $\alpha = 0.75$  (short dashed line),  $\alpha = 0.5$  (long dashed line),  $\alpha = 0.25$  (short dash-dotted line), and  $\alpha = 0.0$  (dotted line).

no secondary oscillations, and a matter power spectrum which appears to match the observation extremely badly both in amplitude and shape.<sup>2</sup> The computed value for  $\sigma_8 \approx 0.42$ —reasonably close to the measured value—and that for  $G\tilde{\mu} \approx 2.0 \times 10^{-6}$ , which implies that  $G\mu \approx 1.0 \times 10^{-6}$  once small-scale structure is taken into account. This is well within the constraint imposed by the absence of timing residuals in the observations of millisecond pulsars [53].

We should emphasize that the predictions of these two simple assumptions are not definitive. They appear to have very similar predictions on large scales, but their predictions on smaller scales are very different, for example, very different values of  $\sigma_8$ . At this stage it seems sensible to consider the implications of both models and hopefully future work will enable us to pin down the predictions of these scenarios more fully.

### III. COMBINING THE SPECTRA AND ITS OBSERVATIONAL CONSEQUENCES

#### A. Combination by a weighted average

At first sight it may appear that combining the effects of adiabatic fluctuations created by inflation and those created actively by topological defects is a highly non-trivial task and indeed if, for example, one were trying to create CMB sky maps by considering the evolution of each mode, it would be. However, computations are simplified considerably by the fact that, at this stage, we are only trying to

compute the power spectra. Since each of the two sources are uncorrelated—one happening during the inflationary epoch and the other after—one can simply add the correctly normalized spectra together.

The only subtle aspect is to normalize each of the two contributions so that the sum is normalized relative to COBE. If one assumes, for the moment, that the normalization of each of the components is arbitrary and to be computed from the observations, one can add the spectra as

$$C_{\ell}^{\text{tot}} = \alpha C_{\ell}^{\text{adia}} + (1 - \alpha) C_{\ell}^{\text{str}},$$

$$P^{\text{tot}}(k) = \alpha P^{\text{adia}}(k) + (1 - \alpha) P^{\text{str}}(k), \quad (21)$$

where  $0 \leq \alpha \leq 1$  is an arbitrary constant defining the relative normalization,  $C_{\ell}^{\text{adia}}$  and  $P^{\text{adia}}(k)$  are the spectra from adiabatic perturbations individually normalized to COBE, and  $C_{\ell}^{\text{str}}$  and  $P^{\text{str}}(k)$  are those for strings. In a specific high energy physics motivated model, for example, the one discussed in Sec. II B, the relative normalization of the two components will be fixed by the parameters of the model, effectively fixing the value of  $\alpha$ .

As a simple illustration of how to use this prescription for combining the spectra, we have computed the angular power spectrum of CMB anisotropies and the power spectrum of the matter fluctuations in the CDM for the standard CDM scenario combined with both the standard scaling source (results presented in Fig. 4) and the standard string model (Fig. 5), for  $\alpha = 1.0, 0.75, 0.5, 0.25$ , and  $0.0$ . These figures illustrate the generic qualitative behavior that one might expect in these mixed perturbation scenarios.

The value of  $\sigma_8$  can be computed from  $P(k)$  via the formula

<sup>2</sup>Both of these deficiencies can be rectified by the inclusion of a cosmological constant with  $\Omega_{\Lambda} \approx 0.7 - 0.8$  (see, for example, Ref. [15]).



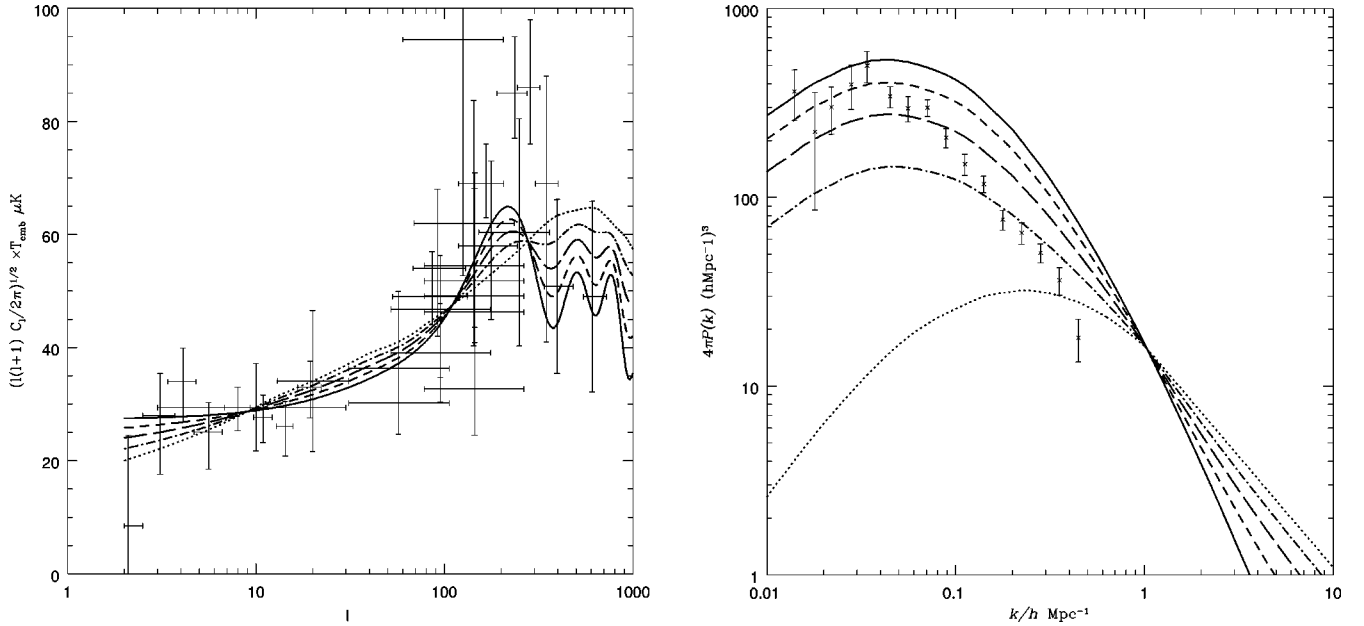


FIG. 5. On the left the angular power spectrum of CMB anisotropies and on the right the power spectrum of fluctuations in the CDM for the standard CDM scenario mixed with standard string source using a ratio of  $\alpha=1.0$  (solid line),  $\alpha=0.75$  (short dashed line),  $\alpha=0.5$  (long dashed line),  $\alpha=0.25$  (short dash-dotted line), and  $\alpha=0.0$  (dotted line).

$$\sigma_8^2 = 4\pi \int \frac{dk}{k} k^3 P(k) |W(8kh^{-1} \text{Mpc})|^2, \quad (22)$$

where the window function  $W(x)$ , given by  $W(x) = 3(\sin x - x \cos x)/x^3$ . Hence, its value in these mixed perturbation scenarios is given by

$$\sigma_8^2 = \alpha(\sigma_8^{\text{adia}})^2 + (1-\alpha)(\sigma_8^{\text{str}})^2, \quad (23)$$

where  $\sigma_8^{\text{adia}}$  and  $\sigma_8^{\text{str}}$  are the COBE normalized values for the individual components. Therefore, we see that the values of  $\sigma_8$  add in quadrature weighted by the factors  $\alpha$  and  $1-\alpha$ . If one of the computed values for the individual components is below the observed value and the other is above, then it is possible to choose  $\alpha$  so that the mixture gives the observed value,  $\sigma_8 \approx 0.6$ . For the combination of standard CDM and the standard scaling source, we find that the value of  $\alpha$  which does this is  $\alpha \approx 0.20$ , whereas for the standard string model  $\alpha \approx 0.15$ . Both these values are low reflecting the fact that on small scales the strings dominate, and hence on the larger scales where the strings appear to be deficient, the appealing aspects of the adiabatic perturbations are lost. We shall see in the next section that this is a robust feature of models using the standard cosmological parameters.

### B. General hybrid inflation models combined with strings

In this section we will discuss qualitatively the observational consequences of allowing for a string induced component to the CMB anisotropies and the fluctuations in the CDM, in addition to an adiabatic component which is assumed to come from inflation. Our treatment is totally general, applying to any inflationary scenario, but specifically we have in mind the GUT scale hybrid inflation scenario

discussed in Sec. II A. We will allow for the moment for the ratio of the two components to be arbitrary and for the spectral index to vary in the range  $0.7 < n < 1.3$ . From the observational point of view, we will start conservatively with simple tests which compare the amplitude of fluctuations in the CMB and the matter distribution, before discussing the shape of the observed power spectrum. Initially, we will concentrate on a universe with critical matter density with a matter content which is comprized only of CDM and baryons. We will see that even with the extra string induced component under discussion here it is difficult to fit all the data without relaxing either of these assumptions.

The COBE normalized spectra of the CMB and CDM for adiabatic component are presented in Fig. 6 for a range of values of  $n$ , and clearly none of the models does particularly well with respect to all the observations. The models with low  $n \approx 0.8$  give a good fit to the observed matter power spectrum, assuming no bias, while giving an apparently poor fit to the observations of the anisotropy in the CMB on small angular scales. For larger values of  $n \approx 1.2$ , the situation is reversed with the fit to the matter power spectrum requiring some kind of scale dependent bias, while at least on smaller angular scales the comparison with the measurements of the CMB is much better, although we note that the large angle spectrum is only marginally compatible with the spectrum of anisotropies detected by COBE. It is this rather unsatisfactory situation, which leads joint analyses of the two different types of measurements to conclude that the best fit to the data is given by something close to  $n=1$ .

Probably the most stringent and robust constraint on any model for structure formation comes from comparing the magnitude of the CMB anisotropies detected by COBE with the amplitude of the measured matter fluctuations on  $8h^{-1} \text{Mpc}$ ,  $\sigma_8$ . Assuming that we can estimate the observed

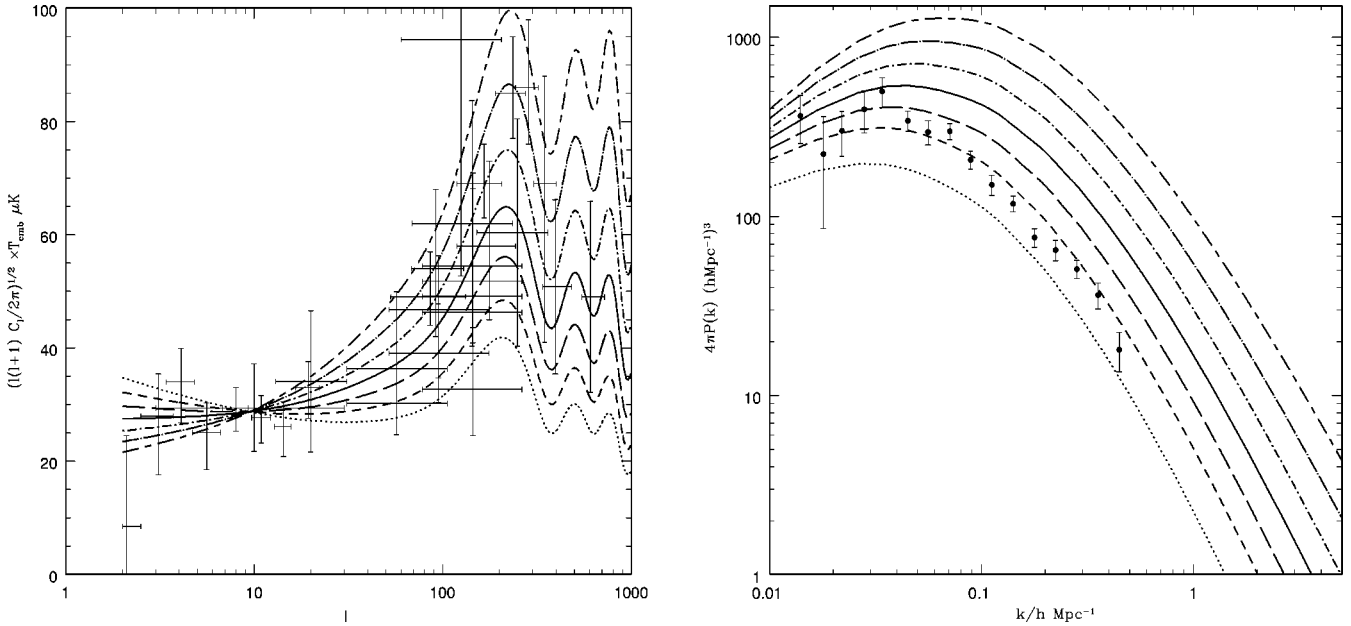


FIG. 6. On the left the angular power spectrum of CMB anisotropies and on the right the power spectrum of the fluctuations in the CDM for models with the spectral index  $n$  varying between 0.7 and 1.3.  $n=0.7$  (dotted line),  $n=0.8$  (short dashed line),  $n=0.9$  (long dashed line),  $n=1.0$  (solid line),  $n=1.1$  (dot-short dashed line),  $n=1.2$  (dot-long dashed line),  $n=1.3$  (short dash-long dashed line). At this stage no string induced component has been included.

value of  $\sigma_8$  in the underlying matter distribution, without recourse to bias or anti-biasing, then it is possible to rule out a large class of models. In particular, as we have already discussed this test would rule out the standard CDM scenario, unless an exotic anti-biasing mechanism was at work.

We will assume, from the point of view of this exercise, the observed value of  $\sigma_8=0.6$  and we will attempt to construct COBE normalized models which can fit this value. This can be done simply by computing  $\alpha$  using Eq. (23) for given values of  $\sigma_8^{\text{adia}}$  and  $\sigma_8^{\text{str}}$ . The computed values of  $\alpha$  are given in Table II for both the standard scaling and string scenarios, and the resulting CDM power spectra are presented in Fig. 7. We see that, in both cases, the spectrum is dominated by the adiabatic component on large scales and by

TABLE II. The computed values of  $\sigma_8$  for pure adiabatic models using the standard cosmological parameters, and a varying spectral index  $n$ . Included also are the values of the ratio  $\alpha$  of the adiabatic and string induced components, if a such a model is to give the observed value of  $\sigma_8 \approx 0.6$  in a critical density universe. The value  $\alpha_1$  is the ratio when the string induced component is that of the standard scaling source, that is,  $\sigma_8^{\text{str}} \approx 0.31$ , and  $\alpha_2$  is that for the standard string source, that is,  $\sigma_8^{\text{str}} \approx 0.42$ .

$n$	$\sigma_8^{\text{adia}}$	$\alpha_1$	$\alpha_2$
0.7	0.62	0.92	0.88
0.8	0.77	0.53	0.44
0.9	0.95	0.33	0.25
1.0	1.18	0.20	0.15
1.1	1.47	0.13	0.09
1.2	1.82	0.08	0.06
1.3	2.25	0.05	0.04

the string induced component on small scales, with the transition taking place around  $k \approx 0.2h \text{ Mpc}^{-1}$ . While the amplitude of  $\sigma_8$  is fitted exactly, the shape of mixed power spectra does not correspond to that which is observed. One could argue that the observations on large scales are much less certain than the amplitude of  $\sigma_8$  and that such models will only be ruled out once more accurate data is available on scales greater than around  $20h^{-1} \text{ Mpc}$ . We should note that there is an interesting qualitative difference between using the standard scaling source and the standard string source on small scales, we shall discuss this phenomenon further in Sec. III D.

It appears that it is not possible to fit the exact shape of the observed power spectrum by just varying the spectral index in a universe with the standard cosmological parameters. A better fit to the current observations may be achieved by varying the cosmological parameters namely the Hubble constant  $h$  the number of massive neutrinos  $N_\nu$ , and the contributions to the cosmological density from CDM  $\Omega_c$ , hot dark matter (HDM) such as neutrinos  $\Omega_\nu$ , the baryonic matter  $\Omega_b$ , and the vacuum energy in the form of a cosmological constant  $\Omega_\Lambda$ . A recent analysis of pure adiabatic models [35] varying these parameters suggests that the models whose parameters are tabulated in Table III along with the computed values of  $\sigma_8$  (included also is the standard cold mark matter scenario) give the best fit to the current observations. The anisotropies in the CMB and the fluctuations in the CDM are plotted in Fig. 8. Note that models B, C, D, and E all fit the shape of the observed matter power spectrum very much in contrast to model A, but that in models B and D anti-biasing, that is, a bias of less than one (in fact,  $b_{\text{CHDM}} \approx 0.85$  and  $b_{\Lambda\text{CDM}} \approx 0.7$ ), is required to reconcile the amplitude of the spectrum with that of the observations (in

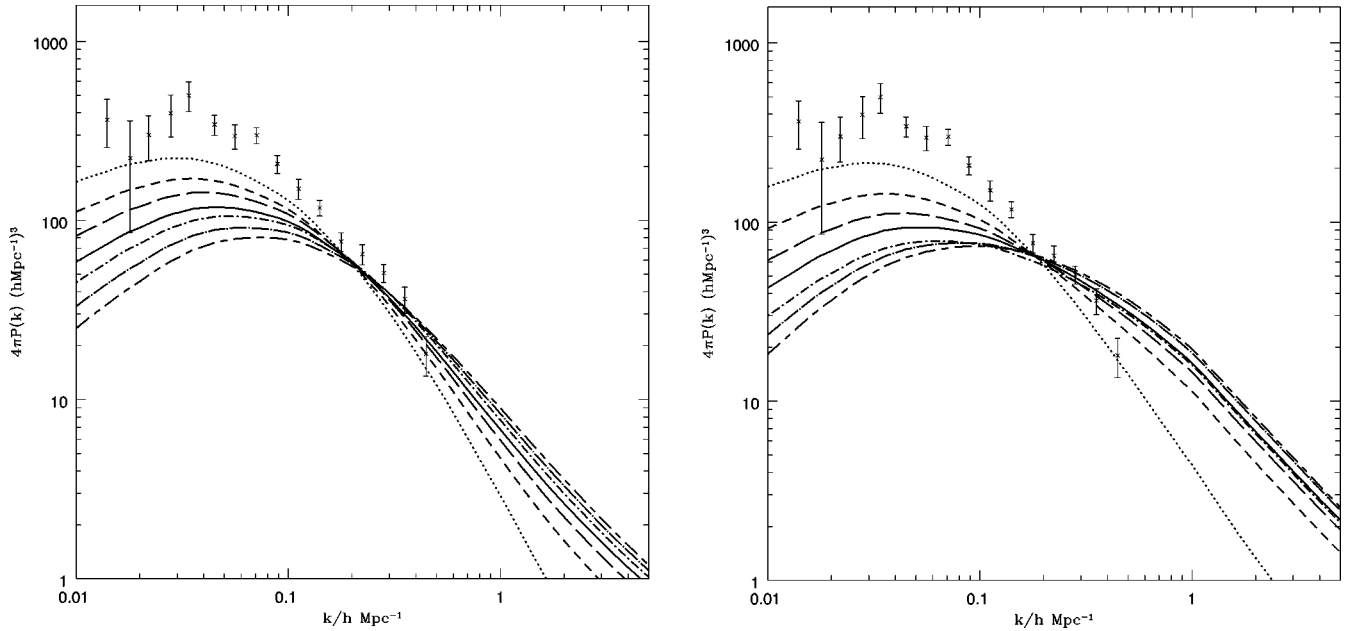


FIG. 7. Mixed perturbation scenarios which require no bias to fit the observed value of  $\sigma_8$  with  $n$  varying between 0.7 and 1.3 for the adiabatic component. On the left the defect component is that of the standard scaling source and on the right it is that of the standard string source. The curves are labeled as in Fig. 6.

Refs. [44,45], the bias of IRAS galaxies was assumed to be one which means that they are good tracers of the underlying mass distribution. This may not necessarily be true).

We have already discussed the inclusion of a string induced component to model A, and models C and E appear to fit the data extremely well without any modifications, but the anti-biasing required for models B and D to fit the data could be perceived as a problem for such scenarios. However, the inclusion of a defect induced component (from either the standard scaling source or the standard string source) with the correct amplitude,  $\alpha=0.7$  for model B and  $\alpha=0.5$  for model D, has exactly the desired effect on large scales, as shown in Fig. 9.

In summary, therefore, the introduction of this extra degree of freedom allows us to fix exactly the amplitude of  $\sigma_8$ , relaxing any constraint on  $n$  from the simple test of comparing the amplitude of CMB anisotropies with  $\sigma_8$ , but this is at the expense of having too little power on large scales. In fact, if one only uses this simple test, there is probably very little constraint on the initial power spectrum on large scales, since the strings can account for the CMB anisotropies observed by COBE. However, if one allows for a small com-

ponent of HDM or a non-zero cosmological constant, then it is possible to fit all the observational data without the need to postulate any kind of bias between the observations and the computed CDM power spectrum. It is also worth noting that each of these mixed scenarios does much better on large scales than the string induced spectrum by itself, mildly relieving the so called “ $b_{100}$  problem” [9,10]. We will discuss the important features of the CMB power spectrum induced in these models in Sec. III E.

### C. Observational aspects of the Linde-Riotto model

We will now turn our attention to the specific supergravity-inspired model of inflation discussed in Sec. II B. There, it was shown that for  $\kappa$  small the predictions were very similar to that of a model with scale-free spectrum, but that for larger values of  $\kappa < \kappa_c$  more exotic initial spectra were possible. We also noted that for generic symmetry breaking schemes the model would lead to the production of cosmic strings whose mass per unit length would be large enough for them to have a substantial effect on cosmic structure formation. If one considers these models as candidates for the mixed perturbation scenarios parametrized by the relative normalization  $\alpha$ , then the normalization of the strings will be given by

$$\frac{G\mu}{1 \times 10^{-6}} \approx \sqrt{1-\alpha}, \quad (24)$$

and the normalization of the adiabatic perturbations requires that

$$1.7 \times 10^{-5} \sqrt{\alpha} \approx \frac{\gamma^2}{\kappa^{3/2}} \left[ \sin\left(\frac{30\kappa}{\pi}\right) \right]^{1/2} \left[ \cos\left(\frac{30\kappa}{\pi}\right) \right]^{3/2}. \quad (25)$$

TABLE III. The cosmological parameters of the models whose CMB anisotropies and CDM fluctuations are plotted in Fig. 8.

Model	Description	$\Omega_c$	$\Omega_b$	$\Omega_\nu$	$\Omega_\Lambda$	$h$	$n$	$N_\nu$	$\sigma_8$
A	SCDM	0.95	0.05	0.00	0.00	0.5	1.0	0	1.18
B	CHDM	0.70	0.10	0.20	0.00	0.5	1.0	1	0.83
C	TCDM	0.90	0.10	0.00	0.00	0.5	0.8	0	0.69
D	$\Lambda$ CDM	0.45	0.05	0.00	0.50	0.6	1.0	0	1.03
E	hCDM	0.95	0.05	0.00	0.00	0.3	1.0	0	0.68

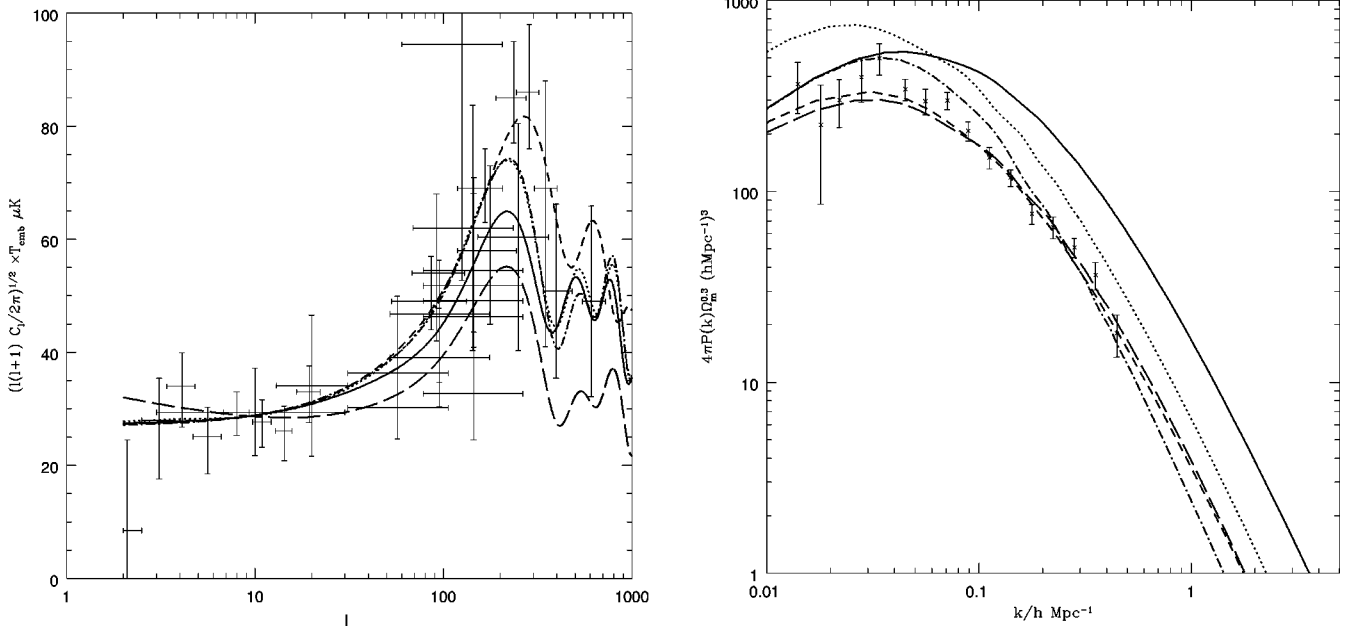


FIG. 8. On the left the angular power spectrum of CMB anisotropies and on the right the power spectrum of fluctuations in the CDM for the best fit CDM type models whose parameters are tabulated in Table III. These models are designed to fit the shape of the observed power spectrum, but note that some of the models (B and D) require anti-biasing to fit the amplitude. (A, solid line) SCDM, (B, dot-short dash line) CHDM, (C, long dashed line) TCDM, (D, dotted line)  $\Lambda$ CDM and (E, short dashed line) hCDM. In both cases the current observational data points are also included to guide the eye.

The value of  $G\mu$  can be computed in terms of  $\gamma$  and  $\kappa$  and therefore one can use Eq. (24) to eliminate  $\gamma$ , to give  $\alpha$  in terms of  $\kappa$ ,

$$\alpha^{-1} = 1 + 0.36\kappa \left[ \sin\left(\frac{30\kappa}{\pi}\right) \cos^3\left(\frac{30\kappa}{\pi}\right) \right]^{-1}. \quad (26)$$

This function can be approximated in both the limit of  $\kappa$  small, in which case  $\alpha \approx 1$ , and  $\kappa \approx \kappa_c$  where  $\alpha \approx 0$ . In these two limiting cases one or the other of the two sources dominates, but in the more general case any relative normalization of the two components is possible. The precise function  $\alpha(\kappa)$  is plotted in the range  $0 < \kappa < \kappa_c$  in Fig. 10 and it is tabulated for various values of  $\kappa$  in Table IV along with the values of  $G\mu$ ,  $\gamma$ , and  $\sigma_8$  for the mixed scenario. Notice that all the values of  $\gamma$ , which can be computed by using the energy units  $E = M_p / \sqrt{8\pi} = 2.4 \times 10^{18}$  GeV, lie in the sensible range of  $1.9 \times 10^{15}$  GeV for  $\kappa = 0.08$  and  $4.6 \times 10^{16}$  GeV for  $\kappa = 0.15$ , and that the corresponding values of  $G\mu$  are even more favorable relative to the constraint from millisecond pulsars [53].

Using this relative normalization and the standard string source model for the defect induced component, we have computed the CMB anisotropies and fluctuations in the CDM for the same values of  $\kappa$  used in Fig. 2 and the properly normalized results are presented in Fig. 11. Notice that the models with large values of  $\kappa$  (for example,  $\kappa = 0.15$ ), which were wildly at odds with the observations without the inclusion of the string induced components, appear to have much more acceptable spectra, with all the computed values of  $\sigma_8$  being around 1. Of course the shape of the spectrum is not quite correct, a feature which is common to most sensible

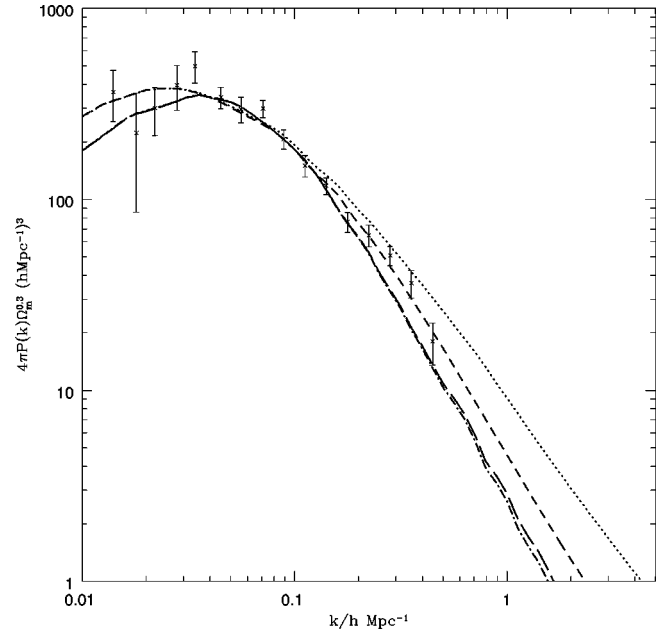


FIG. 9. The power spectrum of the fluctuations in the CDM for models B and D, with a string induced component computed using the standard scaling source (dot-short dashed line and short dashed line, respectively) and the standard string source (long-dashed line and dotted line, respectively). For model B,  $\alpha = 0.7$ —70% adiabatic fluctuations and 30% from strings, while for model D,  $\alpha = 0.5$ —equal proportions of adiabatic and string induced fluctuations. It is clear that each of these models fits the observations very well in the linear regime,  $k < 0.2h \text{ Mpc}^{-1}$ , without the need for bias.

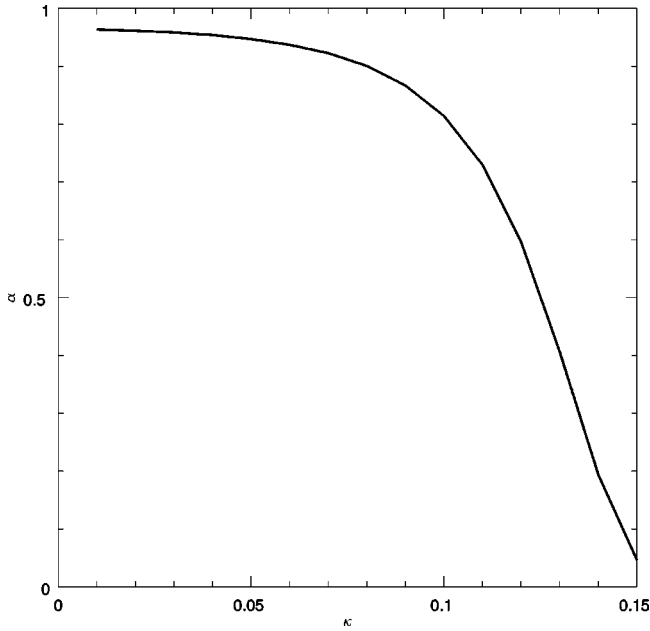


FIG. 10. The relative normalization of the adiabatic and string induced components  $\alpha$  in the Linde and Riotto model plotted as a function of the model parameter  $\kappa$ . The case of  $\alpha \approx 1$  corresponds to most of the fluctuations being adiabatic, and  $\alpha \approx 0$  corresponds to most of them being induced by strings.

critical density CDM models — although, see models C and E from Sec. III B — but it is possible to rectify this situation by the inclusion of a small HDM component or a non-zero cosmological constant. Figure 12 shows the same models using the standard cosmological parameters except that in one we have replaced some of the CDM with HDM ( $\Omega_\nu = 0.3$  and  $N_\nu = 1$ ) and in the other it has been replaced by a non-zero cosmological constant ( $\Omega_\Lambda = 0.6$ ). These are the kind of modifications to the cosmological parameters which are well known to achieve a better fit to the data. However, in the particular case of this inflationary model which generically induces a blue initial spectrum, the amount of HDM or cosmological constant required to achieve a good fit is slightly larger than in the scale free case. We find that the best fit for these models is achieved for the CHDM model with  $\kappa = 0.14$  and for the CDM with a cosmological constant ( $\Lambda$ CDM) it is  $\kappa = 0.13$ . It is interesting to note that, without

TABLE IV. The relative contribution from adiabatic and string induced fluctuations  $\alpha$  as a function of  $\kappa$  for the Linde-Riotto model. Also included are the corresponding values of  $G\mu$  and  $\gamma$  and the value of  $\sigma_8$  using a mixed perturbation scenario with the computed value of  $\alpha$ .

$\kappa$	$\alpha$	$G\mu$	$\gamma$	$\sigma_8$
0.08	0.90	$3.2 \times 10^{-7}$	$8.0 \times 10^{-4}$	1.20
0.10	0.81	$4.4 \times 10^{-7}$	$1.1 \times 10^{-3}$	1.25
0.12	0.60	$6.3 \times 10^{-7}$	$1.4 \times 10^{-3}$	1.28
0.13	0.41	$7.7 \times 10^{-7}$	$1.6 \times 10^{-3}$	1.23
0.14	0.19	$9.0 \times 10^{-7}$	$1.8 \times 10^{-3}$	1.11
0.15	0.05	$9.7 \times 10^{-7}$	$1.9 \times 10^{-3}$	0.99

the string induced component, these models would clearly be at odds with the observations, requiring substantial anti-biasing to be compatible with the observed matter power spectrum and not having anything close to a flat CMB power spectrum on small scales.

#### D. Novel features in matter power spectrum on small scales

So far the discussion of these mixed perturbation scenarios has focused on the linear part of the power spectrum ( $k < 0.2h \text{ Mpc}^{-1}$ ) and the fixing the value of  $\sigma_8$ . In this section, we will focus our attention on the behavior of the power spectrum on small scales when a defect component is included. Investigating these small scales is fraught with complications since the power spectrum will be affected by non-linearity, but methods exist to use the linear spectra that we have computed in the previous sections without resorting to numerical N-body simulations. These methods have been extensively tested using numerical codes for adiabatic models and we shall assume that one can also use them in the case of active fluctuations created by defect networks.

The basic feature that we will use is that the linear power spectra created by defects has much more small scale power than an adiabatic model with the same cosmological parameters. The basic reason for this being that the power spectrum of the strings falls off very slowly inside the horizon, that is,  $\langle \Theta_{00}(k, \eta) \Theta_{00}^*(k, \eta) \rangle \propto k^{-2}$ , whereas the adiabatic perturbations are created at horizon crossing with a sharp tail. Hence, there will be a feature in the power spectrum at some scale, which marks the transition from the spectrum being dominated by adiabatic perturbations to string induced perturbations being dominant. Schematically it can be thought of as a kink in the spectrum, although as one can see from all the figures presented to date for these mixed scenarios it is often difficult to see it clearly with the naked eye. Formally, this corresponds to a change in the fall off of the spectrum on small scales.

We will just illustrate this effect first using the general models which were shown to fit the linear data well in Sec. III B, although this feature also manifests itself in the context of the Linde-Riotto model in almost exactly the same way. Figure 13 shows models B and D with  $\alpha = 0.7$  and  $\alpha = 0.5$ , respectively, as in Fig. 9, but with the adiabatic component and string induced component superposed. Clearly, the mixed spectra deviate significantly from the adiabatic ones on very small scales  $k \approx 1h \text{ Mpc}^{-1}$ , although in the case of model D there is an even noticeable difference on much larger scales around  $k \approx 0.1h \text{ Mpc}^{-1}$ .

Recently, there have been two pieces of observational evidence which might plausibly point to features similar to these in the linear power spectrum. Although it is not totally clear whether these features are artifacts of analysis techniques, it is interesting to broaden the theoretical possibilities under consideration. First, it has been reported that there exists just such a feature in the observed power spectrum [29–31], once the effects of non-linearity have been removed. In these works the authors attempted to explain this feature as being due to complex biasing processes, since no simple CDM variant model appeared to be able to fit the data with

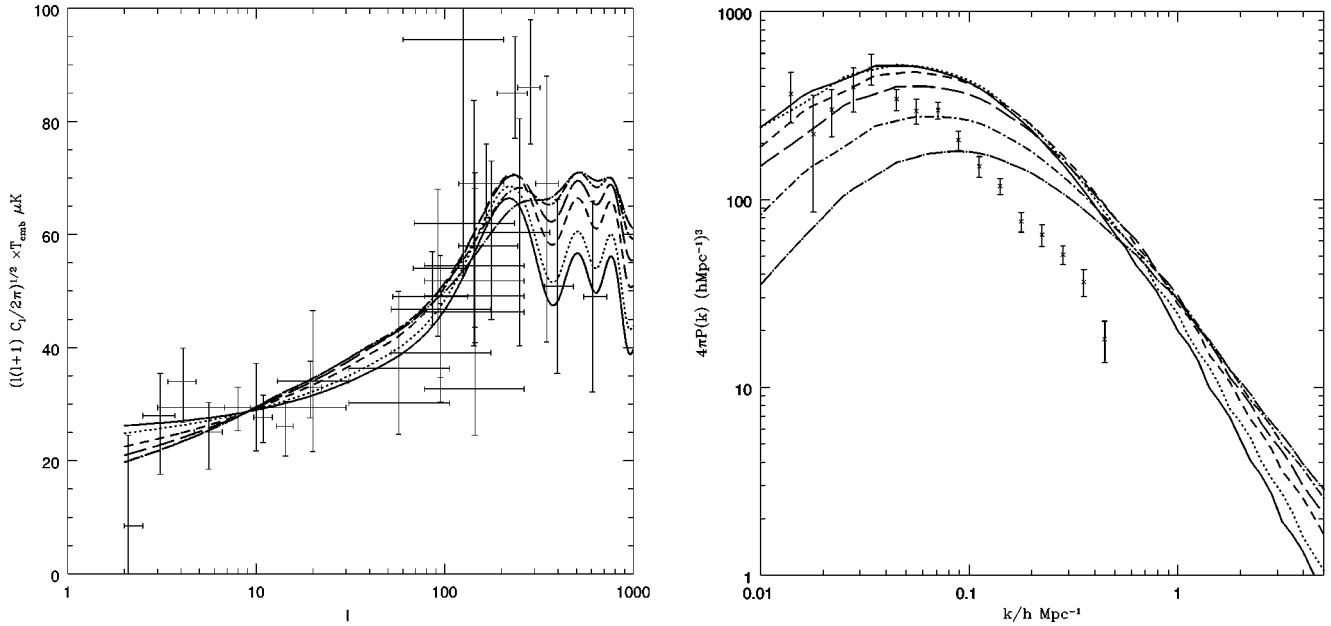


FIG. 11. The same quantities and models as in Fig. 2 except that we have included a string induced component (the standard string source only) with the relative normalization given in Table IV for each value of  $\kappa$ .

just a linear bias. However, here we see that such a feature naturally occurs in these mixed perturbation scenarios which require no bias at all to agree with the observations. We are again assuming that the correct bias of the IRAS galaxies is one. Although this may not necessarily be the case, it does not effect our argument since at the moment we are allowing the relative normalization of the two components to be arbitrary, giving us the freedom to move the large-scale portion of the spectrum up and down. Of course, changing this relative normalization will modify the point at which the

string induced component begins to dominate.

The second piece of observational evidence which might support these kinds of features on small scales is the number of damped Lyman- $\alpha$  systems which are observed at high redshifts ( $z \approx 4$ ). These measurements effectively correspond to an estimate of the same quantity as  $\sigma_8$ , but on much smaller scales. It has been shown that it is difficult to explain the observed amplitude in the context of models such as CHDM (also in TCDM) which fit observations on the larger scales since they produce too little power on small-scales

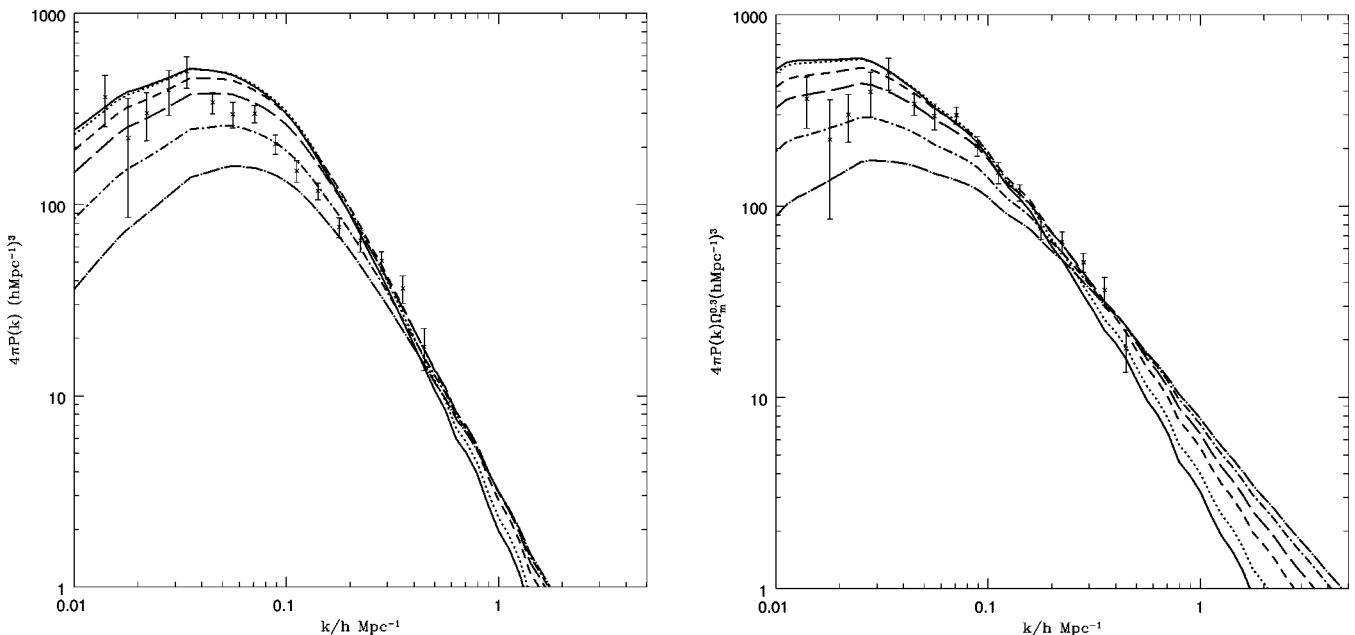


FIG. 12. On the left the CDM power spectrum for the Linde-Riotto model with a string induced component included for  $\Omega_\nu=0.3$  and  $N_\nu=1$ , and on the right for  $\Omega_\Lambda=0.6$ . The curves are labeled as in Figs. 2 and 11. On the left  $\kappa=0.14$  appears to give the best fit whereas on the right  $\kappa=0.13$  is the best. Note that without the inclusion of the string induced component each of these models would be ruled out.

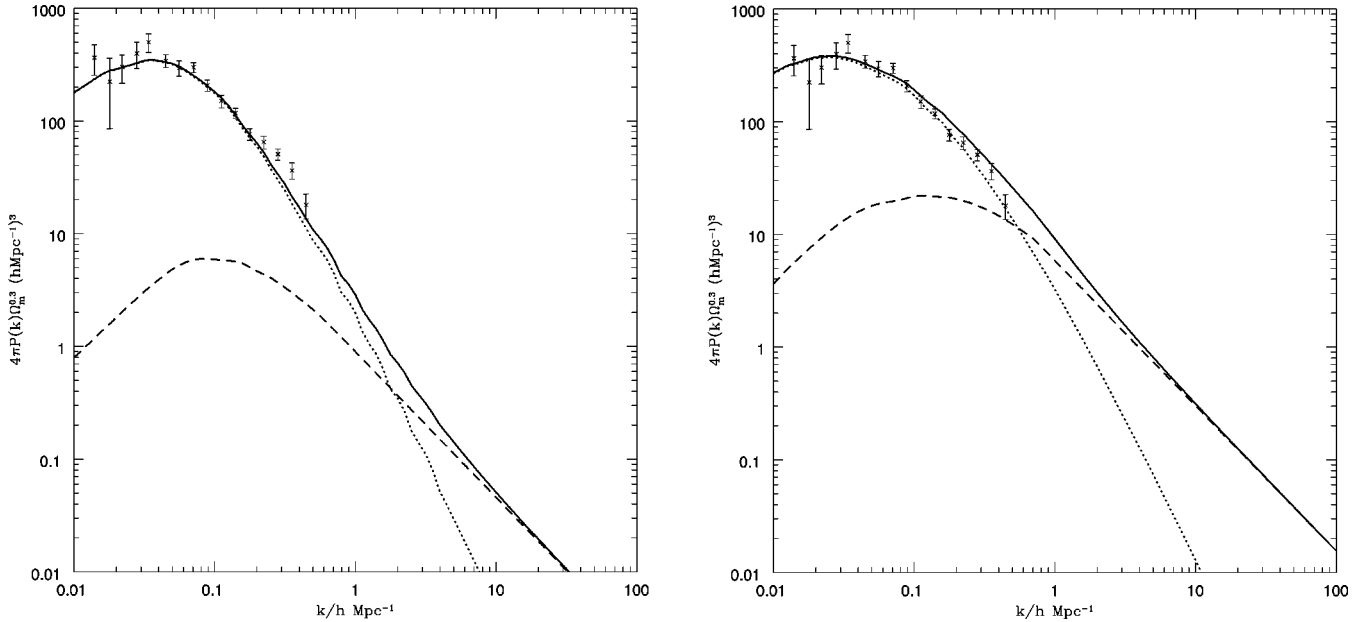


FIG. 13. The same spectra as in Fig. 9. On the left model B with a string induced component and relative normalization of  $\alpha=0.7$ , and on the right model D with a relative normalization of  $\alpha=0.5$ . The spectra are presented over a much wider range of wave numbers than before, and the solid line corresponds to the mixed scenario with the dotted line just the adiabatic component and the dashed line that which is induced by strings. In the case of model D the mixed spectrum deviates significantly from the adiabatic one around  $k \approx 0.5h \text{ Mpc}^{-1}$  and even around  $k \approx 0.1h \text{ Mpc}^{-1}$  there are noticeable effects. Whereas for model B significant deviation from the adiabatic spectrum occur on smaller scales, around  $k \approx 2h \text{ Mpc}^{-1}$ .

(see, for example, Ref. [54] and references therein). Conversely, models such as SCDM which appear to be at odds with the observations on large scales fair much better. Here, we see a simple modification to the model—the inclusion of a defect induced component—which creates more power on smaller scales. The extent to which this can improve the situation for these measurements will be discussed in another publication [55], although it seems clear that given the freedom that we have in these scenarios, it should be possible to fit the data for at least some values of the parameters. It may be that the inclusion of a string induced component can account for the other observations of early structure formation in models which otherwise create too little power.

We should note that both these observational features rely heavily on our ability to continue the power spectrum into the non-linear regime. The comparison with the observations in this regime is much more complicated and less quantitative significance should be attached to these points than the comparison with measurements in the non-linear regime. Nonetheless, they serve as an illustration of the kind of features which these mixed scenarios have. Assuming that the issue of bias can be understood, future redshift surveys (SDSS and 2Df) should be able to make accurate predictions for the power spectrum of the fluctuations in the CDM and hence it will be possible to shed more light on the possible existence of kinks in the power spectrum. In the meantime it seems sensible to investigate further any scenario which naturally has such features.

#### E. Distinctive signatures in the CMB and ruling out mixed scenarios

In the previous sections we have concentrated on the consequences of these mixed perturbation scenarios for the for-

mation of structure, only using the large-angle measurements of the CMB anisotropies to normalize the CDM power spectrum. While the measurements of the CDM power spectrum are relatively extensive from various redshift surveys, the comparison to the computed spectra is always clouded by issues such as bias. Therefore, more clean tests of the cosmological models are required and the measurements of the anisotropies in the CMB on small angular scales should provide more accurate data, free of systematic uncertainties such as bias. The amount of data amassing on smaller angular scales is already substantial and future satellite missions such as Map and Planck should take the study of CMB anisotropies to a new dimension. Therefore, it seems sensible to discuss these possibilities, particularly since we will see that these mixed perturbation scenarios have a very distinctive signature.

The first thing to be aware of in this context is that the spectra for adiabatic models and the active source models under consideration here are very different. The adiabatic spectra generically have oscillations, whereas the active spectra appear not to have these striking features, having just a single rise. Clearly, the superposition of these spectra will have very distinctive features dependent on which of the two components is dominant. The other feature that is very different between the two different types of models is the positions of the maxima in the spectrum. The SCDM model has its maxima around  $\ell \approx 200$ , and all the other flat models have maxima around the same place, but the standard scaling source model does not appear to have an obvious peak in its spectrum and the standard string models have a peak at much smaller scales around  $\ell \approx 500$ .

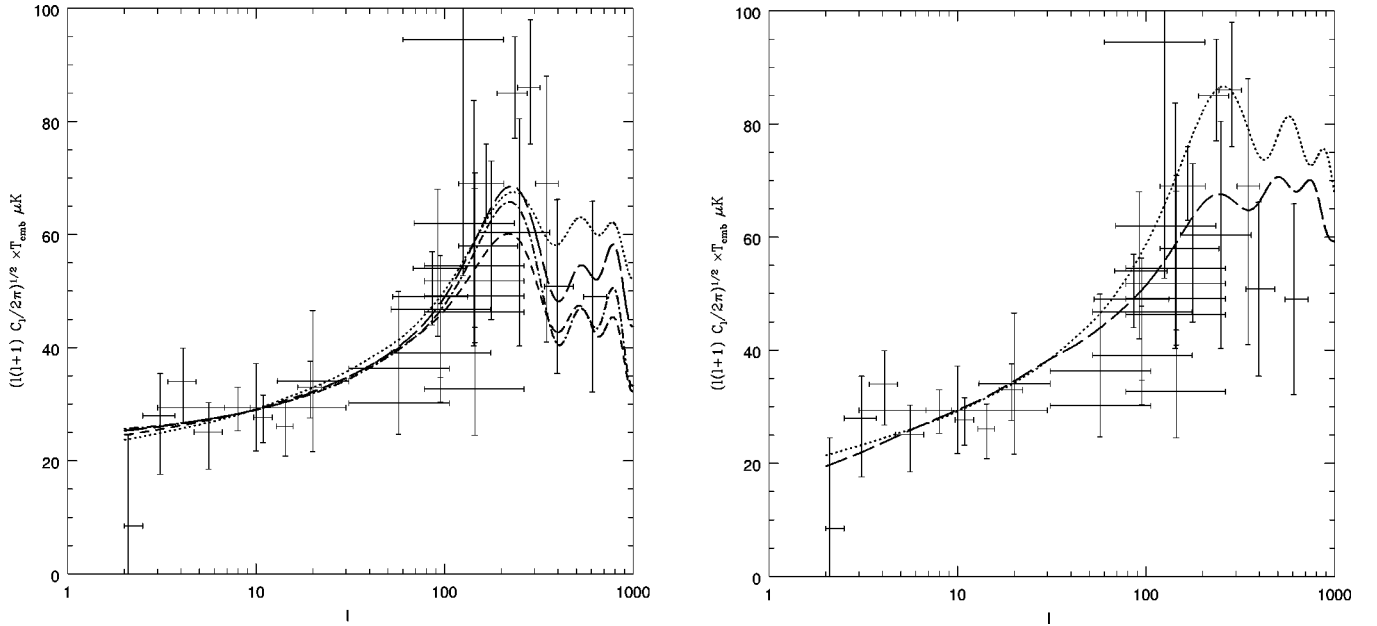


FIG. 14. On the left the CMB anisotropies for the models whose CDM power spectra are presented in Fig. 9. The curves are labeled in the same way as before. On the right are the CMB anisotropies for the Linde-Riotto models which fit the CDM power spectra well. The dotted line has  $\kappa=0.13$  and  $\Omega_\Lambda=0.6$ , and the long dashed line has  $\kappa=0.14$ ,  $\Omega_\nu=0.3$ , and  $N_\nu=1$ .

During the earlier discussions we have illustrated the effects of combining the two types of spectra for very simple cases and it is clear from this that a wide variety of phenomena are possible. To illustrate some of the more important points we have selected the models whose CDM power spectra are presented in Fig. 9 and the Linde-Riotto models which appear to give the best fit to the observations of galaxy clustering by eye from Fig. 12. The CMB anisotropies of these models are presented in Fig. 14.

In the general models, which have a scale free initial spectrum and an arbitrary normalization of the two contributions, the spectra appear to be dominated by the adiabatic fluctuations when the normalization is chosen to give a bias of one relative to IRAS galaxies. When the defect induced component is that of the standard scaling source, then the strings only really contribute on large scales, bringing down the adiabatic component on small scales. Whereas if one uses the standard string source, the opposite is true and the smaller scales ( $l > 400$ ) are boosted relative to models with just the adiabatic component. Of course the first adiabatic peak around  $l \approx 200$  is always suppressed, since both the defect models are relatively low there. It is also interesting to note the behavior of the relative amplitudes of the peaks since in a purely adiabatic model the modulation of the peaks due to baryon drag has been suggested as a test of adiabatic fluctuations [56,57]. Here, we see that the defect component acting as a small background can change the relative sizes for a particular model, which could create confusion when applying this test.

In the models which give the best fit to the data for the Linde-Riotto inflation model, that is, a CHDM model with  $\Omega_\nu=0.3$ ,  $N_\nu=1$  and  $\kappa=0.14$  and a  $\Lambda$ CDM model with  $\Omega_\Lambda=0.6$  and  $\kappa=0.13$ , the CMB anisotropies are dominated by the string induced component on large scales and hence

have a much smaller values of  $\alpha$ . This leads to qualitatively different behavior on smaller scales. The oscillations in the adiabatic component now manifest themselves as undulations on the string induced background, a characteristic feature of these oscillations being the small ratio of the peak to trough height.

It is interesting that we can find models which illustrate both extremes: oscillations modulated by a small background and undulations on a non-oscillatory background. Since we have argued in this paper that none of these possibilities can be ruled out just by purely theoretical arguments, this begs the question how can we rule out or constrain these mixed scenarios. The obvious answer would be to include the parameter  $\alpha$  into any analysis of the CMB data. If we assume, on the basis of the observations of CDM fluctuations on large scales, that at least some of the fluctuations are adiabatic, then it would be interesting to see how close to one  $\alpha$  is. Therefore, it would be an interesting exercise to investigate the potential sensitive of the forthcoming satellite missions to this, and since we have already commented that under some circumstances the inclusion of a defect background can mimic the effects of other cosmological parameters, it appears to be likely that this will introduce yet further degeneracies in the cosmological parameters, which would need to be broken by other measurements.

Although the power spectra that we have discussed extensively in this paper are likely to be most well studied aspects of the future datasets, probably the most characteristic signature of any kind of topological defect is non-Gaussianity. Clearly, the inclusion of an adiabatic component to the power spectrum will make the detection of any kind of non-Gaussianity more difficult, since it will lead to a Gaussian background which would need to be removed before the test for non-Gaussianity is performed. This will no doubt require



more sophisticated and robust tests than are available at the moment, but if these mixed perturbation models are seen to be consistent with future data, then the most compelling argument for their validity over pure adiabatic models, will be the detection of these non-Gaussian signatures.

#### IV. DISCUSSION AND CONCLUSIONS

In this paper we have justified the consideration of models which have two components to the primordial fluctuations, one created by quantum fluctuations during inflation and the other due to a network of evolving topological defects. In places the treatment is totally general, but we have in mind the idea that the production of defects takes place at the end of inflation. We have considered general inflationary models with a constant spectral index and also a specific model based on supergravity which has some very interesting properties, including a spectral index which varies with scale.

In the general case, the inclusion of the string component has some consequences which are similar to those of a tensor component in the CMB anisotropies. In that case the inclusion of an extra component in the CMB allows the matter power spectrum to be pushed down and hence the values of  $\sigma_8$  reduced. However, such models also have problems with large scale power: the SCDM scenario has just about the right amount of power on large scales, but if the spectrum is pushed down substantially then this feature will be lost. These mixed perturbation models also have the same problem and it appears that it is not possible to simultaneously fix the value of  $\sigma_8$  and the shape of the power spectrum on large scales in a universe in which the CDM has a density close to critical matter, even with extreme values of  $n$ . It is, nonetheless, interesting that such models can be made compatible with the simple test of comparing the amplitude of temperature anisotropies measured by COBE and measurements of  $\sigma_8$ .

If one allows for the inclusion of HDM or a non-zero cosmological constant, pure adiabatic models can be fit the observed CDM power spectrum without the need for the inclusion of a component created by strings. However, such scenarios require anti-biasing relative to the IRAS galaxies which are often assumed to be good tracers of the CDM. We have suggested that this may be achieved by the inclusion of a string induced component, although it could equally well be achieved by the inclusion of a tensor component to anisotropy.

The analogy with the inclusion of a tensor component to the anisotropy is not exact, since the strings also contribute to the matter power spectra, albeit at a very low level on large scales. However, on small scales this can have some interesting effects, in particular kinks in the power spectrum and substantial increases in power on very small scales. There is some preliminary evidence that such features may exist and the future large scale redshift surveys, such as

SDSS and 2Df, will hopefully be able to pin this down more accurately. One interesting consequence of the very different behavior of the spectrum on small scales might be that the number of high redshift objects, such as damped Lyman- $\alpha$  systems, might be increased in scenarios such as CHDM which underproduce such systems in the pure adiabatic limit.

In the case of the Linde-Riotto model we saw that if just adiabatic fluctuations were included then the power spectra were wildly at odds with the observations. However, when the string induced component is included the power spectra are much more acceptable, although the inclusion of either HDM or non-zero cosmological constant is necessary to make the shape of the spectrum exactly fit the data.

In whatever inflationary model one considers, these mixed perturbation scenarios have distinct signatures in the CMB. If the adiabatic perturbations dominate, as would have to be the case for a single constant spectral index, the inclusion of a defect component would lead to the modulation of the peak structure, mimicking the effects of baryon drag. While in the models such as that proposed by Linde and Riotto, one finds that the defect component can dominate the CMB anisotropies. In this case the adiabatic oscillations manifest themselves as undulations on the defect spectrum which otherwise has no oscillations. Finally, we suggested that it is a challenge to the forthcoming satellite experiments to confirm or constrain these kinds of scenarios by taking  $\alpha$  as a free parameter to be computed. Since there is no *a priori* reason to believe that these mixed perturbation scenarios can be excluded on any theoretical grounds, such a test would provide a useful information on the nature of physics at high energies.

*Noted added.* During the final stages of this work, we became aware of two other papers which discussed similar ideas [58,59]. Reference [58] follows up the suggestion [20] that a substantial string induced component would be created in the D-term inflation scenario, while Ref. [59] discusses the possibility of string formation as a consequence of open inflation scenarios [60]. Both these works reiterate our general conclusions, but emphasize different aspects.

#### ACKNOWLEDGMENTS

We thank U. Seljak and M. Zaldarriaga for the use of CMBFAST, and A. Albrecht, J. Magueijo, A. Liddle, A. Linde, N. Turok, and R. Jeanerrot for helpful conversations. The model for strings used in this work was developed by R.A.B. in collaboration with A. Albrecht and J. Robinson. We would like to thank them for permission to use these computations in this work. The computations were done at the UK National Cosmology Supercomputing Center, supported by PPARC, HEFCE, and Silicon Graphics/Cray Research. The work of R.A.B. was funded by Trinity College and that of J.W. is supported by DAAD financed by the German Federal Ministry for Research and Technology.

- [1] A. H. Guth, *Phys. Rev. D* **23**, 347 (1981); A. D. Linde, *Phys. Lett.* **108B**, 389 (1982); A. Albrecht and P. J. Steinhardt, *Phys. Rev. Lett.* **48**, 1220 (1982).
- [2] T. W. B. Kibble, *J. Phys. A* **9**, 1387 (1976).
- [3] A. Vilenkin and E. P. S. Shellard, *Cosmic Strings and Other Topological Defects* (Cambridge University Press, Cambridge, England, 1994).
- [4] M. Hindmarsh and T. W. B. Kibble, *Rep. Prog. Phys.* **58**, 477 (1995).
- [5] Ya. B. Zel'dovich, *Mon. Not. R. Astron. Soc.* **192**, 663 (1980).
- [6] A. Vilenkin, *Phys. Rev. Lett.* **46**, 1169 (1981); **46**, 1496(E) (1981).
- [7] U. Seljak and M. Zaldarriaga, *Astrophys. J.* **469**, 437 (1996).
- [8] U. L. Pen, U. Seljak, and N. Turok, *Phys. Rev. Lett.* **79**, 1615 (1997).
- [9] A. Albrecht, R. A. Battye, and J. Robinson, *Phys. Rev. Lett.* **79**, 4736 (1997).
- [10] A. Albrecht, R. A. Battye, and J. Robinson, *Phys. Rev. D* **59**, 023508 (1999).
- [11] B. Allen, R. R. Caldwell, S. Dodelson, L. Knox, E. P. S. Shellard, and A. Stebbins, *Phys. Rev. Lett.* **79**, 2624 (1997).
- [12] C. Contaldi, M. Hindmarsh, and J. Magueijo, *Phys. Rev. Lett.* **82**, 679 (1999).
- [13] A. Albrecht, R. A. Battye, and J. Robinson (unpublished).
- [14] P. P. Avelino, R. R. Caldwell, and C. J. A. P. Martins, *Phys. Rev. D* **56**, 4568 (1997).
- [15] R. A. Battye, J. Robinson, and A. Albrecht, *Phys. Rev. Lett.* **80**, 4847 (1998).
- [16] P. P. Avelino, E. P. S. Shellard, J. H. P. Wu, and B. Allen, *Phys. Rev. Lett.* **81**, 2008 (1998).
- [17] L. Kofman, A. Linde, and A. A. Starobinskii, *Phys. Rev. Lett.* **76**, 1011 (1996).
- [18] I. Tkachev, S. Khlebnikov, L. Kofman, and A. Linde, *Phys. Lett. B* **440**, 262 (1998).
- [19] A. Linde, *Phys. Lett. B* **259**, 38 (1991); A. Linde, *Phys. Rev. D* **49**, 748 (1994).
- [20] R. Jeannerot, *Phys. Rev. D* **53**, 5426 (1996).
- [21] D. H. Lyth and A. Riotto, *Phys. Rep.* **314**, 1 (1999).
- [22] A. Linde and A. Riotto, *Phys. Rev. D* **56**, 1841 (1997).
- [23] C. J. A. P. Martins and E. P. S. Shellard, *Phys. Rev. D* **54**, 2535 (1996).
- [24] K. M. Gorski, A. J. Banday, C. L. Bennett, G. Hinshaw, A. Kogut, G. F. Smoot, and E. L. Wright, *astro-ph/9601063*.
- [25] E. F. Bunn and M. White, *Astrophys. J.* **480**, 6 (1997).
- [26] J. R. Bond, A. H. Jaffe, and L. Knox, *astro-ph/9808264*.
- [27] J. R. Bond and A. H. Jaffe, *astro-ph/9809043*.
- [28] B. J. Carr, J. H. Gilbert, and J. E. Lidsey, *Phys. Rev. D* **50**, 4853 (1994).
- [29] J. A. Peacock, *astro-ph/9606151*.
- [30] J. A. Peacock, *astro-ph/9805208*.
- [31] C. Smith, A. Klypin, M. Gross, J. Primack, and J. Holtzmann, *astro-ph/9702049*.
- [32] A. D. Linde, *Phys. Lett.* **129B**, 177 (1983).
- [33] E. P. S. Shellard and R. A. Battye, *astro-ph/9801115*; R. A. Battye and E. P. S. Shellard, *Phys. Rev. Lett.* **73**, 2954 (1994); **76**, 2203(E) (1994); R. A. Battye and E. P. S. Shellard, *Nucl. Phys.* **B423**, 260 (1994).
- [34] J. Garcia-Bellido and A. Linde, *Phys. Lett. B* **398**, 18 (1997).
- [35] E. Gawiser and J. Silk, *Science* **280**, 1405 (1998).
- [36] P. Fayet and J. Iliopoulos, *Phys. Lett.* **51B**, 461 (1974); E. D. Stewart, *Phys. Rev. D* **51**, 6847 (1995).
- [37] J. A. Casa, J. W. Moreno, C. Munoz, and M. Quiros, *Nucl. Phys.* **B328**, 272 (1989); E. Halyo, *Phys. Lett. B* **387**, 43 (1996); P. Binetruy and G. Dvali, *ibid.* **388**, 241 (1996).
- [38] E. J. Copeland, A. R. Liddle, D. H. Lyth, E. D. Stewart, and D. Wands, *Phys. Rev. D* **49**, 6410 (1994).
- [39] G. Dvali, Q. Shafi, and R. K. Schaefer, *Phys. Rev. Lett.* **73**, 1886 (1994).
- [40] G. Lazarides, R. K. Schaefer, and Q. Shafi, *Phys. Rev. D* **56**, 1324 (1997).
- [41] A. Linde (private communication).
- [42] D. H. Lyth, *hep-ph/9609431*.
- [43] The data points have been compiled by M. Tegmark at <http://www.sns.ias.edu/max/cmb/experiments.html>.
- [44] J. A. Peacock and S. J. Dodds, *Mon. Not. R. Astron. Soc.* **267**, 1020 (1994).
- [45] J. A. Peacock and S. J. Dodds, *astro-ph/9603031*.
- [46] T. W. B. Kibble, *Nucl. Phys.* **B252**, 227 (1985); **B261**, 750(E) (1985).
- [47] A. Albrecht and N. Turok, *Phys. Rev. D* **40**, 973 (1989).
- [48] D. Bennett and F. Bouchet, *Phys. Rev. D* **41**, 2408 (1990).
- [49] B. Allen and E. P. S. Shellard, *Phys. Rev. Lett.* **64**, 119 (1990).
- [50] G. R. Vincent, M. Hindmarsh, and M. Sakellariadou, *Phys. Rev. D* **55**, 573 (1997).
- [51] A. Vilenkin (private communication).
- [52] B. Carter, *Phys. Rev. Lett.* **74**, 3098 (1995).
- [53] R. R. Caldwell, R. A. Battye, and E. P. S. Shellard, *Phys. Rev. D* **54**, 7146 (1997).
- [54] D. J. Eisenstein and W. Hu, *astro-ph/9710252*.
- [55] R. A. Battye, J. Magueijo, and J. Weller, *astro-ph/9906093*.
- [56] W. Hu and M. White, *Phys. Rev. Lett.* **77**, 1687 (1996).
- [57] W. Hu and M. White, *Astrophys. J.* **471**, 30 (1996).
- [58] C. Contaldi, J. Magueijo, and M. Hindmarsh, *Phys. Rev. Lett.* **82**, 2034 (1999).
- [59] P. P. Avelino, R. R. Caldwell, and C. J. A. P. Martins, *Phys. Rev. D* **59**, 123509 (1999).
- [60] A. Vilenkin, *Phys. Rev. D* **56**, 3258 (1997).